

Development of a Standard for Structural Testing of Implants in Transfemoral Osseointegrated Prostheses

Emilia Öhr
Sofie Ludvigsson

2016



LUND
UNIVERSITY

Integrum

Master's Thesis in Biomedical Engineering

Faculty of Engineering LTH
Department of Biomedical Engineering

Supervisor: Ingrid Svensson, Department of Biomedical Engineering.
Assistant supervisors: Max Ortiz Catalan & Marta Björnsdóttir, Integrum AB.

Preface

This Master's Thesis has been conducted as part of a Master of Science in Biomedical Engineering at the Faculty of Engineering, Lund University. The thesis project has been carried out at Integrum AB, Gothenburg, between January and June 2016. The aim of this project was to develop a standard for structural testing of implants in transfemoral osseointegrated prostheses, since there is a lack of ISO standards regarding this type of implants.

First of all, we would like to thank Max Ortiz Catalan, assistant supervisor at Integrum AB, for giving us the opportunity to do this thesis project within the interesting and pioneering field of osseointegrated implants. We also wish to thank Marta Björnsdóttir, also assistant supervisor at Integrum AB, who has given us valuable input during this project and encouraged us in our work.

We would also like to thank our supervisor at Lund University, Ingrid Svensson, who has been very helpful and supportive throughout the processes.

During this project, we got the opportunity to visit the walking school for amputees, *Gåskola*, at Sahlgrenska University Hospital in Gothenburg. A special thanks to Kerstin Hagberg for showing us around and increasing our insight in the rehabilitation process.

At last, but not least, we wish to thank Patrik Stenlund for his time and the load cell data that he provided us with, from his time as a Ph.D. student at the Department of Biomaterials, University of Gothenburg. His contribution was very valuable for this project.

Abstract

The aim of this Master's Thesis was to develop a standard for structural testing of implants to be used in transfemoral osseointegrated prostheses, since there is a lack of such standards for this type of implant. The methods used in this project include a literature study, a review of ISO standards, simulations of gait in a software called OpenSim, and a comparison of the OpenSim results with measurements from a load cell. Equivalent stresses in the implants were also calculated for both the OpenSim and load cell data, to establish the test values for the standard and to evaluate the worst case scenario.

From the results it was concluded that the implants should be tested for compression, bending and torsion, in a cyclic test that simulates gait. A static test corresponding to more severe loading situations, such as stumbling or falling, should also be considered. The results from OpenSim were consistent with the load cell data to some extent, despite that the simulations were based on normal gait while the measurements were taken from amputees using osseointegrated prostheses. Because of this, the OpenSim results were not found suitable to use in the developed standard, and the test values for the cyclic test were therefore based on the load cell data.

Further development opportunities of the outcome of this project include improving the OpenSim models, completing the standard, performing more extensive load cell studies, and testing the developed standard practically.

Keywords: transfemoral amputation; osseointegrated prostheses; structural testing; OPRA; gait; simulations; OpenSim; Integrum AB.

Terminology

Abutment	The skin penetrating part of the OPRA implant system, connecting the prosthesis to the implanted fixture.
Abutment screw	The part of the OPRA implant system that locks the abutment to the fixture.
Fixture	The anchoring element of the OPRA implant system, which is inserted and integrated in the patient's bone.
OPRA	Osseointegrated Prostheses for the Rehabilitation of Amputees. <i>Integrum AB's</i> implant system for osseointegrated lower and upper limb prostheses, which consists of three different components: an abutment, an abutment screw and a fixture.
Osseointegration	A method for direct anchoring of titanium implants to bone, through ingrowth of bone cells into the implant.
Transfemoral	Across the femur (thigh bone).

Contents

1	Introduction	1
1.1	Background	1
1.2	Problem definition	2
1.3	Goal and purpose	2
1.4	Structure of the report	3
1.5	Division of work	3
2	Theory:	
	Biomechanical Concepts	5
2.1	Anatomical terms	5
2.2	Lower limb anatomy	5
2.3	Gait cycle	6
2.4	Mechanical loading modes	7
3	Theory:	
	The OpenSim Software	11
3.1	OpenSim models	11
3.2	The Gait 2392 model	13
3.3	OpenSim analyses	14
4	Theory:	
	Lower Limb Prosthetics	15
4.1	Conventional socket prostheses	15
4.2	Osseointegration	15
4.3	The OPRA implant system	16
5	Methodology	19
5.1	Literature study	19
5.2	Review of ISO standards	19
5.3	OpenSim simulations	20
5.4	Comparison to load cell data	23
5.5	Equivalent stress calculations	27

5.6	Determination of test forces	29
6	Results	33
6.1	Literature study	33
6.2	Review of ISO standards	34
6.3	Data analyses:	
	OpenSim simulations and load cell data	36
6.4	Equivalent stress calculations	40
6.5	Determination of test forces	48
7	Discussion	51
7.1	Literature study	51
7.2	Review of ISO standards	52
7.3	OpenSim simulations	52
7.4	Comparison: OpenSim, load cell, and article data	57
7.5	Assumptions and limitations in OpenSim	61
7.6	Determination of test forces	62
7.7	Ethical reflection	64
8	The Developed Standard	65
8.1	Scope	65
8.2	Terms and definitions	65
8.3	Test principle	66
8.4	Materials	66
8.5	Apparatus	67
8.6	Test parameters	68
9	Conclusions	71
9.1	Further work	72
	Bibliography	75
	List of Figures	79

1. Introduction

Osseointegrated prosthetics as a treatment for lower limb amputees is a relatively new method, and *Integrum AB* is world leading in the development of the technology [1]. There are however different systems being developed around the world, and the competition is increasing. Because it is a quite young field, there is a lack of standards regarding testing of the implants used for attachment of the prostheses. Therefore, in order to make sure an implant meets the requirements posed on it, and withstands the loads it is subjected to in everyday life, there is a need for development of a standard for structural testing.

1.1 Background

In the year of 1990, the first patient in the world was treated with a trans-femoral osseointegrated prosthesis, in a surgery performed by Dr. Per-Ingvar Brånemark and Dr. Björn Rydviik. A few years later, in 1998, *Integrum AB* was founded by Per-Ingvar Brånemark and Rickard Brånemark [1]. *Integrum AB* will from here on be referred to as *Integrum* in this report.

Integrum is based in Gothenburg, Sweden, and their treatment method called the OPRA implant system (see Figure 1.1), is today being used in 12 different countries. The company is expanding and on the 16th of July 2015, the OPRA implant system was approved by the *U.S. Food and Drug Administration* (FDA). *Integrum* is thereby the first company in the world with a bone anchored prosthesis on the U.S. market [1].

Since the first surgery in 1990, the OPRA implant system has been used to treat more than 400 patients around the world. It has been used for both lower and upper limb amputations, and for various amputation levels. There are 25 years of experience behind the OPRA implant system used today, and several clinical studies have proven the benefits patients can gain from using the system [1]. However, since the technique is still relatively new, there are no international standards for mechanical testing of the implants similar to those available for other orthopaedic implants, e.g. hip implants.

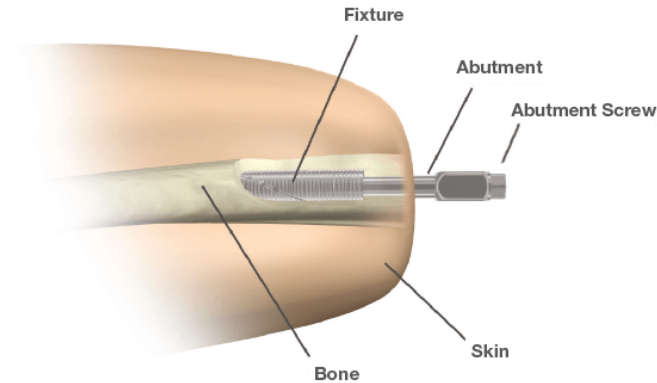


Figure 1.1: Illustration of the OPRA implant system.
Copyright by Integrum AB, used with permission.

1.2 Problem definition

Optimising the mechanical strength of the OPRA implant system is important for preventing over- or under-designing of the various components, which could make them inefficient or unsafe to use [2]. Different components need to have different strength; the fixture is not allowed to break under any circumstances, while the abutment screw is the weakest link and should deform if the patient for example falls on it [3]. An abutment that is too compliant might risk fracturing and transferring the impact onto the fixture, or bending too much which might make attachment and detachment of the prosthesis difficult. A too stiff abutment on the other hand, might increase the risk of fracturing the femur or the implant-bone interface since the load is transferred directly onto the residuum [4].

For further development of osseointegrated prostheses, a better understanding of the loads an implant is subjected to and how this can be simulated and tested, is required. It is necessary to develop a standardised method for testing the implants mechanically, in order to ensure that each implant meets the load bearing requirements posed on it in everyday life. Since the loading is significantly higher in lower limb prostheses compared to upper limb prostheses, the lower limb is in focus when it comes to developing the mechanical tests.

1.3 Goal and purpose

In order to make sure each transfemoral implant has the desired mechanical properties, an appropriate test method and rig is required. The purpose of this

Master's Thesis was to contribute to the development of this, by working with two goals. The first goal was to develop a standard for performing realistic structural tests of osseointegrated transfemoral implants. The second goal of the project involved designing a functional prototype of a test rig to be used for these tests.

1.4 Structure of the report

This report is divided into nine chapters. The first chapter has given an introduction to *Integrum* and the OPRA implant system. This chapter has also presented a problem definition, as well as the goal and purpose of this project. Chapter two, three and four provide theory; knowledge on which this thesis is based upon. Thereafter, in chapter five, the methodology that has been used in this project is described. In the sixth chapter the results are presented, and in the seventh chapter these are discussed, together with an ethical reflection on the topic. Chapter eight contains the developed test standard, and in the ninth and final chapter conclusions about the project and the results are drawn, and future development opportunities are discussed. This is followed by a Bibliography and List of Figures.

1.5 Division of work

The authors of this thesis have both been involved in all parts of the project, and the report has been written in collaboration. However, S. Ludvigsson has focused more on the OpenSim and MATLAB coding, while E. Öhr has concentrated more on interpreting results.

2. Theory:

Biomechanical Concepts

2.1 Anatomical terms

In the field of biomechanics, anatomical planes are often used to describe locations of structures and directions of motion, in relation to the standard anatomical position illustrated in Figure 2.1. Anatomical planes are theoretical planes dividing the human body into different parts, and there are three main planes. For each plane there are terms for describing locations and motions.

- The ***sagittal plane***: divides the body into a left and a right part. Terms for describing positions in this plane are *anterior*, meaning towards the front, and *posterior*, meaning towards the backside.
- The ***frontal plane***: divides the body into a front and a back part. In this plane, *medial* means towards the midline, and *lateral* means away from the midline.
- The ***transverse plane***: divides the body into an upper and a lower part. *Superior* is used for describing above, and *inferior* is used for below.

These planes and terms are illustrated in Figure 2.1. Other terms that are useful, especially when it comes to limbs, are *proximal* and *distal*. They refer to location in relation to the trunk: proximal means towards the trunk, and distal means away from the trunk. When referring to a femur (thigh bone), the proximal end is located at the hip and the distal end at the knee [5].

2.2 Lower limb anatomy

Figure 2.2 shows an illustration of the human lower limbs. The main bones of the leg are the femur, the tibia, the fibula and the patella. The femur is the longest bone in the human body; the proximal end articulates with the acetabulum in the pelvic bone and forms the hip joint, and the distal end articulates with the tibia and the patella and forms the knee joint [5].

Lower limb amputation can occur at many different levels, and they can be transtibial or transfemoral. This project focuses on transfemoral amputations, meaning when the amputation has been made somewhere along the femur.

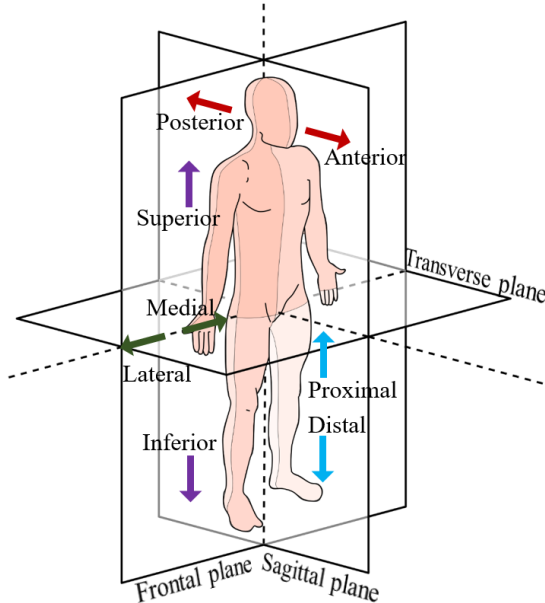


Figure 2.1: Anatomical planes and related terms.

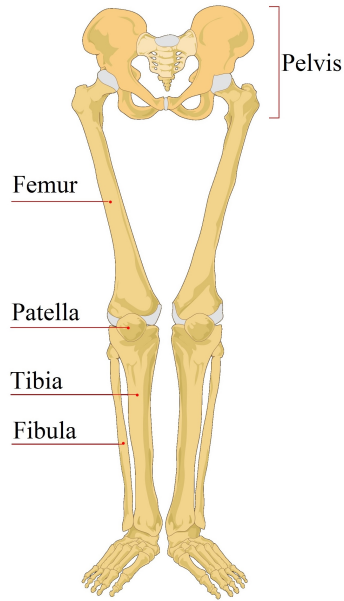


Figure 2.2: Anatomy of the human lower limbs.

2.3 Gait cycle

Gait, i.e. walking, involves complex interactions among a range of major joints in the body; in the lower limbs in particular, but also in the rest of the body. It is a cyclic activity consisting of two major phases for each lower limb: stance and swing. The stance phase begins with the heel strike and ends with the toe-off. The swing phase is the period that follows when the toes have left the ground, until the heel of the same foot strikes again. There is a slight overlap of the stance phase of one foot and the swing phase of the other; the toe-off of the left foot comes shortly after the heel strike of the right foot, and vice versa. During this overlap, the body is supported by both limbs, and this period is therefore called double support. One stride or cycle is defined as a whole stance phase and a whole swing phase of the same leg, i.e. from heel strike of one foot until the beginning of the subsequent heel strike of the same foot [6].

In general, the stance phase corresponds to 60% of the stride. The phase can be divided into six events: heel strike, loading response, midstance, terminal stance, pre-swing and toe-off. These events are illustrated in Figure 2.3. Heel

strike is defined as the instant the foot makes contact with the ground, and this is also called initial contact. Loading response is the part where the whole sole of the foot comes in contact with the ground, and the weight of the body is transferred onto the supporting limb. This is followed by midstance, during which the whole body weight is supported by one limb, and the tibia of this limb rotates over the foot in the direction of locomotion. After midstance the body weight is transferred onto the forefoot, during the terminal stance period. This is followed by the pre-swing period, during which the body weight is transferred over to the contralateral limb. The pre-swing ends with the toe-off, which is the instant when the foot leaves the ground [6].

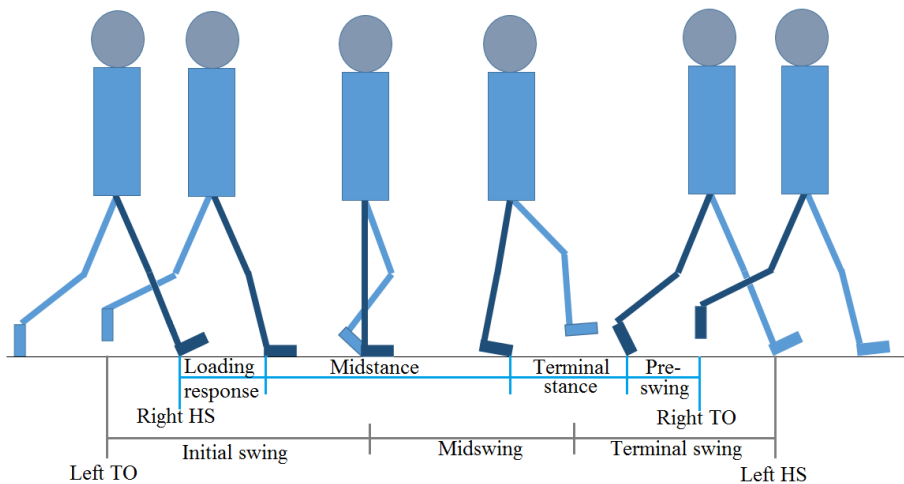


Figure 2.3: Illustration of the stance and swing phases during gait. HS is short for heel strike, and TO means toe-off.

The swing phase makes up 40% of the gait cycle, and it can be divided into three periods: initial swing, midswing and terminal swing. These periods are also illustrated in Figure 2.3. The initial swing lasts from toe-off until the swinging foot is next to the supporting foot, at which point the midswing starts. Midswing ends when the tibia of the swinging limb is oriented vertically, and the terminal swing lasts from this point until heel strike [6].

2.4 Mechanical loading modes

Different mechanical loading modes will affect the objects they are acting on differently. The behaviour of the subjected object will vary depending on the direction of the applied load, as well as if the loading is static or cyclic [7].

2.4.1 Direction of loading

An applied load can either be axial (compressive or tensile), bending, torsional, or a combination of these (multiaxial). These different modes of loading are further explained below:

- **Axial load:** When an object is loaded with an axial load, the force is directed towards or away from the surface of the structure, thereby causing a normal stress which can be either compressive or tensile.
- **Bending load:** During bending, the object is subjected to a transverse loading. When the object is bent, it causes tensile stress on the convex side and compressive stress on the concave side. During exposure to bending, stress and strain are maximal at the surface of the object and are zero along its neutral axis.
- **Torsional load:** An object that is subjected to torsional loading is being twisted, causing shear stress to develop.
- **Multiaxial load:** When an object is exposed to multiaxial load, the loading is applied multidirectionally and is a combination of the modes described above. This type of loading is often hard to record due to its complexity.

Living bone is seldom loaded in one direction only and for this reason neither is an implant that is integrated in the bone. *In vivo* measurements on bone have demonstrated the complexity of multiaxial loading during walking and jogging. The measurements show that during one gait cycle, the bones in a leg are subjected to compressive and tensile forces, as well as shear and torsional forces [7].

2.4.2 Static and cyclic loading

An applied load can either be static or cyclic. Depending on what type is used for a mechanical test, the test will reveal different aspects of the material's strength [7].

- **Static loading:** a load that is applied with a constant force for a period of time. It can reveal what load an object can tolerate prior to fracture, as well as the ultimate strength of the material, i.e. the maximum stress [7].
- **Cyclic loading:** a load that is applied repetitively at a certain frequency during a period of time. A repetitive load can cause microdamages to occur in the subjected object. The damages accumulate with each cycle as the intensity of the testing, i.e. the magnitude of the load or the number

of cycles, increases [7]. For all structural metals, this can cause failure of the material at loads below the ultimate strength. This type of failure, which is often what is investigated using cyclic tests, is called fatigue [8].

3. Theory:

The OpenSim Software

OpenSim is an open-source software, created for musculoskeletal modelling and dynamic movement simulation [9]. It allows for building and analysing of models, as well as exchanging of experiences through the related online forum [10]. The software is developed and distributed by *the NIH National Center for Simulation in Rehabilitation Research* (NCSRR), through their site *www.simtk.org* [11]. For this project, version 3.3 was used. The software is targeted towards biomechanical scientists, clinicians and developers [12]. OpenSim can be used to simulate numerous different scenarios and perform a variety of different analyses, and it is therefore a complex program. The basic knowledge needed to understand how the program has been used in this project is provided below.

3.1 OpenSim models

An OpenSim model represents a system of rigid bodies that are connected through joints, i.e. a skeleton, and acted upon by forces to produce motion. Each model is described by a *.osim*-file, written in an XML code structure. When the software is downloaded, a number of example models are included. There are also a number of models created by other users to be found in the online forum associated with the program. Regardless of where a model is found or if it is created from scratch, it is made up by the same set of components: bodies, joints, forces, markers, constraints, contact geometries and controllers. The first four components are the main ones that will be explained below. Each of these represents a different part of the system and has different properties. They can be edited either in the graphical user interface (GUI), where they are found in the Navigator window, or using a separate XML editor such as *Notepad++* [12]. A screenshot of the GUI is presented in Figure 3.1.

Bodies

The bodies in an OpenSim model are rigid bodies representing skeletal parts and the surrounding tissue. They are contained in the model's BodySet. Prop-

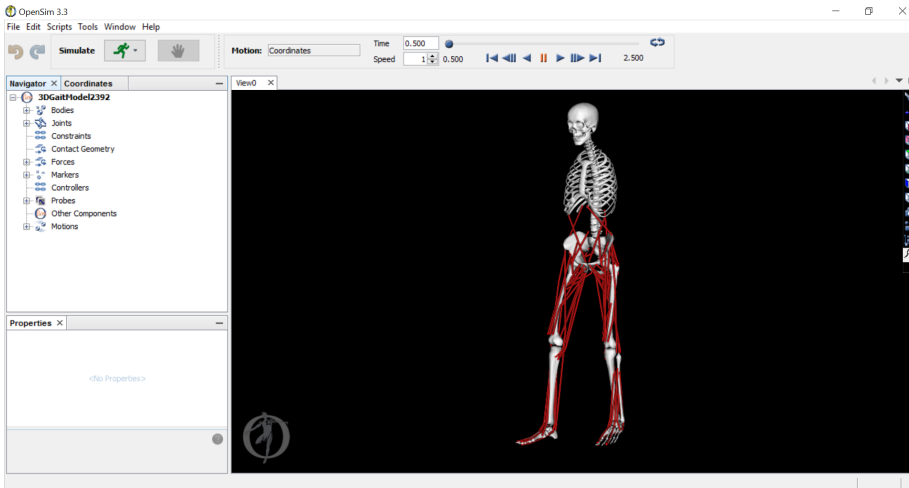


Figure 3.1: Screenshot of the OpenSim 3.3 GUI.

erties that are specified and can be edited in the model include mass, centre of mass, moments of inertia, and a `VisibleObject`. The `VisibleObject` contains a geometry file, which specifies what the body will look like in the GUI [12].

Joints

Each body is connected to one or several other bodies through joints. A joint defines the coordinates and kinematic transforms that make up the relative motion between the connected bodies. In OpenSim there are six types of joints, and an additional `CustomJoint` that can be defined according to the need of the user. Joint properties describe the location of the joint in the two bodies it connects, the orientation of these bodies and coordinates in which the joint can move [12].

Forces

In order to set the bodies of the model in motion, application of forces is needed. These forces are defined in the `ForceSet`-section of the model. There are different types of forces that can be applied, one of which is muscle force. Further, OpenSim contains various different muscle models. They all include properties such as a set of points defining where the muscle is connected to the bodies, maximum force that can be generated, and optimal muscle fibre length [12].

Markers

In order to simulate the model using a motion recorded experimentally, and perform analyses on it, virtual markers are needed. They should be placed so

that they represent the location of the experimental markers that were used for data recording. All markers are defined in the model's MarkerSet. Properties that are specified for a marker include its name, at what body in the model it is placed, and its location in relation to that body. The name of the marker must match the name of the corresponding marker in the experimental data [12].

3.2 The Gait 2392 model

One of the example models that are included in the OpenSim software package is the *Gait 2392* model. It is a human musculoskeletal model that can be used for simulation of gait. The model's BodySet includes a torso and a pelvis, and for each of the lower limbs: a femur, tibia, talus, calcaneus, and toe body. The joints included in the lower extremities are the hip, knee, ankle, subtalar and metatarsophalangeal joints. A total of 76 muscles in the lower extremities and torso are included in the model, and the default version represents a person who is 1.80 m tall and weighs 75.16 kg [12]. A screenshot of the model from the OpenSim GUI can be seen in Figure 3.2.

In addition to the actual model, the *Gait 2392* model package also includes experimental data from a gait analysis, as well as set-up files for performing various analyses in the software [12].

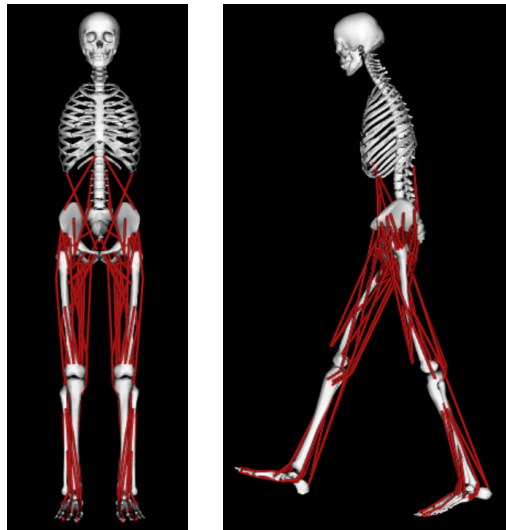


Figure 3.2: Screenshot from OpenSim 3.3 of the *Gait 2392* model in its default pose (left), and in motion (right).

3.3 OpenSim analyses

There are a number of different analysis tools available in OpenSim. The ones that are covered by the scope of this thesis are Inverse Kinematics, Static Optimization and Joint Reactions analysis. These are briefly described below.

Inverse Kinematics

The Inverse Kinematics (IK) tool uses experimentally recorded data of a movement, e.g. gait, and positions the model to achieve the best possible fit of the model's markers to the experimental markers. This is done for each time frame of the recorded data, and the best fit is said to be the pose that minimises a sum of weighted squared errors of the markers' positions. To perform the analysis, OpenSim needs three inputs: the model (*.osim*-file), the experimental marker trajectories (*.trc*-file), i.e. the paths of the markers during the motion, and a set-up file (*.xml*) containing marker weightings. The marker weightings decide what markers should be prioritised, and markers with higher weightings will be fitted with less error. The IK tool returns a motion file (*.mot*) as output, containing joint angles and/or translations in each of the time frames specified by the experimental data [12].

Static Optimization

Static Optimization (SO) is an analysis tool that calculates the individual muscle forces needed at each instant, in order to create the motion specified in a motion file. This is done by minimizing the sum of squared muscle activations. The inputs needed to perform an SO analysis are: the model (*.osim*-file), a motion file (*.mot*), e.g. the output from an IK analysis, and an *.xml*-file containing external load data, such as ground reaction forces (GRF). For some motions, for example gait, an additional file describing residual actuators needs to be appended to the model. When using IK results as an input, they normally need to be filtered. This can be done directly in OpenSim [12]. The outputs generated from the SO analysis include three files, one of which is a storage file (*.sto*) containing the muscle forces described over time [12].

Joint Reactions Analysis

The Joint Reactions analysis tool (JR) calculates the resultant forces and moments acting at the joints between consecutive bodies, as a result of all loads applied to the model. In order to do this, the same inputs as for SO are needed: the model file, the motion file, external load data and residual actuators. In addition to this, the force file generated by the SO analysis is needed as an input. The analysis will then create a storage file (*.sto*) containing values of three force and three moment vectors (x, y, z) for each joint, described over time [12].

4. Theory:

Lower Limb Prosthetics

4.1 Conventional socket prostheses

The conventional method for attachment of a prosthesis to a transfemoral amputee is by using a socket [13]. The socket is the connecting area between the residual femur and the prosthesis, and it is traditionally made out of a stiff material. A one way valve at the distal end of the socket allows for suspension around the leg through suction [14].

Patients using socket prostheses can experience various socket related problems. Discomfort and pain is one type of issue, including skin problems such as sores and rashes [15]. Limb pain and soft tissue breakdown have also been described to be common [16], as well as heat and sweating in the socket, and discomfort while standing, walking and sitting [17]. Practical complaints include difficulty donning the prosthesis, unreliability of the prosthesis being securely suspended [15], and difficulties related to volume changes of the stump [13]. A third type of issue related to the use of a socket prosthesis is the biomechanical aspect: changes in gait, reduced hip flexion and extension, increased pelvic tilt, and lack of stabilization is commonly experienced among transfemoral amputees wearing conventional prostheses [13].

4.2 Osseointegration

Osseointegration refers to a structural and functional connection between living bone tissue and the surface of a load-bearing artificial implant. The original definition of osseointegration was “a direct structural and functional connection between ordered living bone and the surface of a load-carrying implant” [18]. This has however been modified since the discovery [13], and the definition used today is: “...when there is no progressive relative movement between the implant and the bone with which it has direct contact” [19].

Osseointegration was first discovered and described in the 1950s, by Swedish professor Per-Ingvar Brånemark [13]. The discovery and development of the

technique has revolutionised dental prosthetics. Although dental implants was the initial field of use, many additional applications have emerged during the years. These include bone-anchored prostheses for head and neck defects, bone-anchored hearing aids, finger joint prostheses and thumb amputation prostheses [15]. The method has also proven to be successful in total joint replacement, e.g. for hip and knee arthroplasty [13]. Today new possibilities are still being explored, and osseointegrated lower-limb prostheses is one of the latest areas of use.

There are three basic stages enabling a successful osseointegration: a delicate surgical technique causing minimal damage to the surrounding tissue, a sufficient recovery period allowing for optimal ingrowth of the bone, and a controlled loading of the implant when the use of it begins. Careful rehabilitation and controlled loading allows for bone remodelling around the implant, which results in further integration and enhanced long-term clinical results [13].

4.3 The OPRA implant system

The development of osseointegrated prostheses for transfemoral amputees started in 1990 [20]. In this alternative to conventional prostheses, the socket is replaced by an osseointegrated implant. The method developed at *Integrum*, called the OPRA implant system (*Osseointegrated Prostheses for the Rehabilitation of Amputees*), includes a fixture, an abutment and an abutment screw [15], all made of a titanium alloy [3].

The OPRA implant system, and how it is integrated with the residual limb, is shown in Figure 1.1. The fixture is osseointegrated with the residual bone, and the abutment is attached through a press-fit connection. The abutment screw is inserted to lock the abutment to the fixture and keep the system preloaded [3]. The abutment is the part of the system that penetrates through the skin and allows for attachment of an external prosthesis [21]. The system is available for several different amputation levels, for both upper limbs; transhumeral, transradial and finger/thumb amputations, and lower limbs; transfemoral and transtibial amputations [1].

4.3.1 Target group

The target group for the OPRA implant system is patients who have undergone amputation as a result of trauma or cancer. The treatment is mainly intended for patients having rehabilitation problems with conventional socket prostheses, and patients who cannot use them at all [1]. The patient should not weigh more than 100 kg to be considered a candidate for the OPRA implant system [22].

4.3.2 Benefits for transfemoral amputees

The OPRA implant system has proved to be a successful alternative for transfemoral amputees experiencing problems when using conventional prostheses [21]. Potential advantages of using an osseointegrated prosthesis include reduction of skin problems, alleviation of stump pain and improvement of sensory feedback (osseoperception). Compared to using a socket prosthesis an osseointegrated prosthesis can permit a greater range of hip motion, improved sitting comfort, and a simple attachment and detachment of the prosthesis. In addition it can also enable the amputee to walk further and be more active [2]. Beyond these advantages, the OPRA system also offers a solution for patients who are not able to wear a conventional socket prosthesis due to a high level amputation or severe damage to the stump [13]. Overall, the technique can contribute to a significant improvement in quality of life for transfemoral amputees [2].

4.3.3 Mechanical issues and current solutions

Although osseointegrated fixation of transfemoral prostheses overall is a promising technique, there are some issues left to resolve. Occasional mechanical failure of the implant system has been reported [2], such as cracking, bending, or complete fracturing of the abutment and/or the abutment screw [4]. Previous studies have shown that this can occur as a result of falling, or due to fatigue after extensive use [16]. A less frequently occurring but more severe issue to consider, is mechanical failure of the fixture. This type of failure has greater consequences than damage to the abutment or abutment screw, which are more easily replaced compared to the fixture. For this reason, the abutment and abutment screw are designed to deform or fracture before the fixture does [3]. This feature also protects the implant-bone interface from overloading [2]. However, all damages to the abutment and the abutment screw have both personal, financial and clinical effects and are seen as a shortcoming of the technique [4].

Another potential issue is stress shielding, which is a result of a decrease in stress distribution in the bone caused by the implant. This happens when the implant has a greater mechanical stiffness compared to the bone, and it leads to bone remodelling due to changes in the loading environment [6]. Remodelling of bone can lead to problems such as distal and endosteal bone resorption and changes in the bone structure. In a study from 2012, a radiological assessment of long-term fixation and stability of osseointegrated transfemoral implants was performed to investigate the impact of bone remodelling. The results obtained showed that moderate bone loss and remodelling occurs similarly to what is seen for fully coated femoral stems used in total hip arthroplasty. Apparent distal bone resorption, causing exposure of the fixture, was found in three out of

47 participants at their 2-year follow-up. According to the study, this resorption does not seem to affect the fixation stability or performance of the implants [13]. However, in a long-term perspective, remodelling of bone close to the fixture can lead to implant loosening [16]. A patient who suffers from loosening of their lower limb implant often experiences pain during weight-bearing, and needs to have the implant removed [20].

The current solution for protecting the implant and the residual bone from overloading is the use of a safety device called *OPRA AxorTM II*. It has a release function in bending and torsion, and is there to protect the implant from excessive load [1]. It is often used in combination with a hydraulic knee [4]. *OPRA AxorTM II* is placed between the abutment and the prosthesis, and the release function is triggered if the load in either bending or torsion exceeds a certain threshold [1]. For bending, this threshold is 70 ± 5 Nm, and for torsion it is set to 15 ± 2 Nm [23]. Although this technique works, there is a need for an increased understanding of the load regime experienced by the abutment in daily activities, in order to optimize the strength of the abutment and develop different prosthetic components further [2].

4.3.4 Current test requirements

The mechanical test procedure for the transfemoral OPRA implants used today includes a cyclic fatigue test and a separate torsion test. The cyclic test involves subjecting the implant to high compressive loads and bending moments, for 10 million cycles. The number of cycles is based on the fact that an average amputee walks approximately 1 million gait cycles per year, and by testing for 10 million cycles an implant lifetime of 10 years is simulated. In addition to the compression and bending test, a separate torsion test is performed. In this test, the whole system is subjected to a torsional moment for 5 million cycles. Both tests are performed in a saline solution heated to 37°C, to simulate a biological environment. During the test, the implant is held in place by a gripping device, gripping around the proximal end of the fixture [3].

Today's requirements are based on gait analyses from osseointegrated patients and Finite Element Analyses, but no simulations of the loads occurring during the gait cycle have been performed [3]. In addition, the separate torsion test is not as realistic as if all types of loadings would be performed in one test, since it is known that bones are loaded multiaxially during gait. Further, the test set up using a gripping device might not be the ideal way of simulating osseointegration of the fixture in a residual limb.

5. Methodology

5.1 Literature study

The first part of this project's work process consisted of a literature study. This was carried out with the aim of gaining suitable background knowledge about osseointegrated prostheses and the OPRA implant system, as well as collecting information to base the development of the standard on. The literature studied consisted of scientific papers, some of which were provided by *Integrum* and some of which were found using *LUBsearch*, the Lund University Libraries' search tool for electronic resources. When searching for articles on *LUBsearch*, the following keywords were used: osseointegration; osseointegrated prosthesis; transfemoral amputation; lower limb amputation; OPRA; gait analysis. After going through the matching papers, together with the ones provided by *Integrum*, twelve articles were selected for more exhaustive studying.

5.2 Review of ISO standards

After the literature study, a review of ISO standards was carried out. ISO standards are developed by the *International Organization for Standardization* (ISO), and they provide specifications, requirements or guidelines for a company's products. They are there to ensure quality, efficiency and safety on the international trade market, and make sure materials, products, services and systems are suitable for use. ISO standards cover various different aspects of technology and business, including medical equipment [24]. In this project, the review of ISO standards was performed to gain understanding of what mechanical criteria the implants have to meet in everyday life, how these can be formulated into test conditions, and how the performance of the implants can be evaluated.

ISO standards for implants and prostheses with mechanical behaviour and load bearings similar to those of the transfemoral implants were reviewed. These were found by browsing the ISO standards catalogue, using ICS categorisation (International Classification for Standards). The ICS categorisation means that the standards have been classified into different fields of technology, and the category found the most suitable for reviewing in this project was ICS

11.040.40 – *Implants for surgery, prosthetics and orthotics*. From this category, three standards were selected for further review:

- ISO 10328:2006 *Structural testing of lower-limb prostheses – Requirements and test methods*.
- ISO 7206-4:2010 *Implants for surgery – Partial and total hip joint prostheses – Part 4: Determination of endurance properties and performance of stemmed femoral components*.
- ISO 7206-6:2013 *Implants for surgery – Partial and total hip joint prostheses – Part 6: Endurance properties testing and performance requirements of neck region of stemmed femoral components*.

The first two, ISO 10328:2006 and ISO 7206-4:2010, were already available at *Integrum*, together with an older version of the third standard, ISO 7206-6:1992. Since the newer version of ISO 7206-6 only constituted a minor revision of the old one, the version from 1992 was still found useful and thus further purchasing of standards was not necessary. ISO 7206-6:1992 is called *Implants for surgery – Partial and total hip joint prostheses – Part 6: Determination of endurance properties of head and neck region of stemmed femoral components*.

5.3 OpenSim simulations

The third method used in this project was simulations in OpenSim, which was used to create a musculoskeletal gait model of a person fitted with a transfemoral osseointegrated prosthesis. This model will from here on be referred to as the osseointegrated model or the OI model. The aim of developing the OI model was to simulate what forces and moments the implant has to withstand during gait, and to study how the loading changes with amputation level.

5.3.1 Model development

When developing the OI model, a model found in the OpenSim online forum was used as a starting point [25]. This model represents a transfemoral amputee fitted with a socket prosthesis, and it is based on the *Gait 2392* model described in section 3.2. The major modifications that have been made from the *Gait 2392* model are changes in the BodySet and ForceSet. In the BodySet, the tibia and the bodies of the foot have been removed from the amputated limb (the left leg), in addition to the distal half of the femur in the same limb. The tibia and the foot have been replaced by a prosthetic lower leg and foot, and a socket connecting the remaining femur to the prosthetic lower leg has been

added. Changes that have been made in the ForceSet include removal of all muscles originating from the femur or tibia of the amputated limb and inserting at a more distal bone, as well as shortening of all muscles originating from the pelvis and inserting below the amputation level. The shortened muscles have been reattached at the distal end of the amputated femur.

To create the OI model, a few changes were made to the prosthetic model described above. The prosthetic lower leg and foot were not edited, and initially no changes were made to the ForceSet either. However, the socket part of the prosthesis and how this connected to the rest of the body needed to be altered. In the original prosthetic model, the connection between the socket and femur was defined through a CustomJoint. In the OI model, a different joint type was selected. Since osseointegration is defined as a lack of movement between the implant and the bone it is connected to, a weld joint with no degrees of freedom was chosen to mimic the interface. The joint was tilted so that the long axis of the implant was aligned with the distal end of the residual femur. The geometry file associated with the socket, i.e. the VisibleObject, was also modified to resemble the implant, the *OPRA AxorTM II* and the prosthetic femur. These parts were all modelled as one body, connecting to the amputated femur through the weld joint, and the prosthetic lower leg through the knee joint. The changes in the geometry file were made using a software called *3D Builder*, which was available through Microsoft Windows 10, and the body is from here on referred to as the implant body. The VisibleObject created for this body can be seen in Figure 5.1.

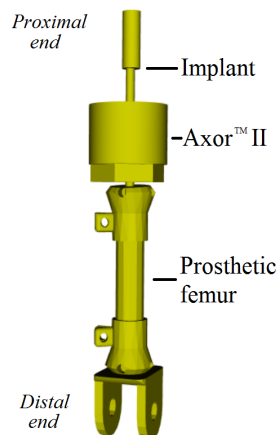


Figure 5.1: Illustration of the VisibleObject associated with the implant body.

In order to fulfil the aim of comparing the loading associated with different amputation levels, the OI model was modified further. The socket prosthesis

model included a femur amputated approximately in the middle of the long axis of the bone, and by modelling two more amputations; one higher and one lower compared to the original one, three OI models were produced. The amputation level was changed through modification of the centre of mass and the geometry file of the amputated femur, as well as those of the implant body. The displacement of the weld joint connecting these bodies, as well as the angle of the joint, were also adjusted. Since the femoral bone is curved, the angle had to be altered with the amputation level in order to keep the implant aligned with the bone. The ForceSet was also modified slightly for the different amputation levels, by adapting the connecting points of the muscles at the distal end of the femur to its new coordinates. A screenshot of the three models, simulating different amputation levels, are shown in Figure 5.2.

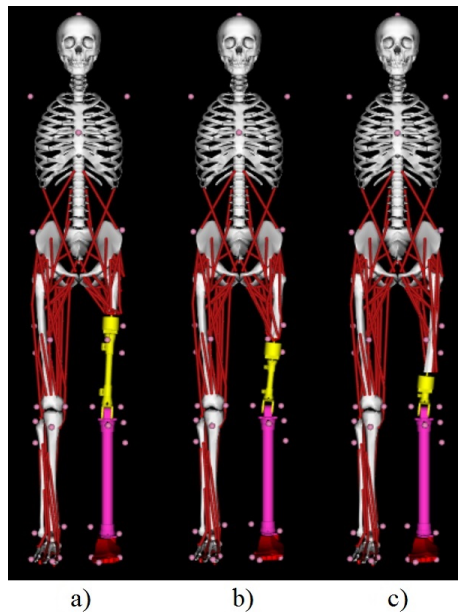


Figure 5.2: A screenshot from OpenSim 3.3 of the OI models of three amputees fitted with osseointegrated prostheses, at different amputation levels:
a) high amputation, b) mid amputation, c) low amputation.

5.3.2 Model analysis

In order to determine what loads the implants are subjected to during walking, three analyses were performed on each of the OI models: Inverse Kinematics (IK), Static Optimization (SO) and Joint Reactions (JR) analysis. These are all described in section 3.3.

For the IK analysis, marker trajectories and weightings associated with the original *Gait 2392* model were used. By observing the gait motion, the timing of one gait cycle was determined to approximately 1.20 - 2.45 seconds. The analyses were thereafter performed on the data for this period.

After performing IK, SO was used to determine the muscle forces at each time frame throughout the cycle. As inputs, the results from the IK analysis were used, together with residual actuators and external load data (ground reaction forces) associated with the *Gait 2392* model. The IK results were filtered by 6 Hz, which is the standard setting for filtering in the OpenSim analysis tool.

For the JR analysis, the same inputs and settings were used as for SO, in addition to the force file generated by the SO analysis. The results files were then exported to MATLAB (MathWorks[®]) for results processing.

5.3.3 Results processing

Using MATLAB, scripts for plotting the results from the JR analysis were created. Each of the force and moment components were plotted in separate figures, with the results of all three models in each of the plots. This resulted in six different plots, two for each of the axes: antero-posterior (AP), long axis (L) and medio-lateral (ML). For all of the plots, the x-axis was set to time normalised to percentage of a gait cycle (%GC), where 0 %GC corresponded to heel strike of the prosthetic left leg, and 100 %GC equalled the subsequent heel strike of the same leg. For the force plots, the y-axis was set to force normalised by the model's body weight (%BW). Similarly for the moment plots, the y-axis was set to moment normalised by the body weight, resulting in a unit of metres (m).

5.4 Comparison to load cell data

In order to evaluate the quality of the results from the OpenSim simulations, the plots of the force and moment components were compared to data collected with load cells. Two sets of gait data were used for comparison, and both were collected from unilateral transfemoral amputees. These subjects performed straight line walking at self selected speed in a clinical environment and a load cell, fitted between the abutment and the prosthesis, measured the forces and moments in three dimensions.

The first data set was found in an article by Lee et al. from 2008 [16]. In this study, a load cell was used to analyse the magnitude and variability of the loading experienced by the implant during walking. This was done for twelve subjects, and the results are presented in plots similar to those created in this

project [16]. For this data set, only the plots have been used for comparison in this project. No raw data has been studied.

The second data set that was used for comparison was collected as part of P. Stenlund's Ph.D. thesis in 2015 [26]. This data was gathered from five subjects, and was used to perform site-specific loading analyses to determine the loads applied on the OPRA implant system and how this affects the bone-implant interface [26]. From this data set, the raw data recorded with the load cell interface [26]. From this data set, the raw data recorded with the load cell was used to perform a comparison with the results from OpenSim. For each of the five subjects, the data from three walks were interpolated and averaged in MATLAB. However, the data from the load cell was collected between the abutment and the prosthesis, which is not the same location as the OpenSim results were plotted for. Therefore, the averaged load cell measurements were used for calculating the values at the same location as was used in OpenSim, see section 5.4.1. Finally, the forces and moments in all three directions were plotted in graphs similar to those presented in the article by Lee et al.

For the rest of this report, load cell data will refer to the data set received from Stenlund. When discussing Lee et al.'s data set, this will be specified.

5.4.1 Transformation of forces and moments in a rigid body

The results from the JR analysis in OpenSim were generated for the weld joint connecting the implant body to the amputated femur. Visually, this joint is located at the proximal end of the fixture, inside the intramedullary canal of the residual femur. However, OpenSim separates visual objects from actual mechanical properties, and due to the nature of a weld joint, this joint is mechanically more similar to the location in the abutment where the distal end of the fixture begins. This segment is illustrated in Figure 5.3, and it is the cross section at this location for which the forces and moments are presented.

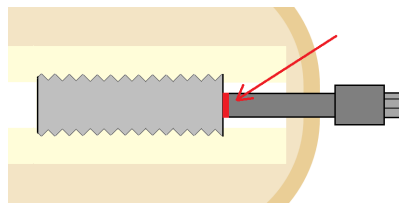


Figure 5.3: Illustration of the segment of the abutment (at the red arrow) for which the forces and moments from the OpenSim JR analysis are given.

The load cell data from Stenlund contains measurements from a location that is at a more distal position than the abutment. Since both the abutment and

the load cell are located within the same rigid body it is however possible to convert the measured forces and moments from the coordinate system of the load cell to the coordinate system of the abutment. A simplified illustration of the forces (F_{AP} , F_L and F_{ML}) and moments (M_{AP} , M_L and M_{ML}) acting on a distal position, and the converted forces (F'_{AP} , F'_L and F'_{ML}) and moments (M'_{AP} , M'_L and M'_{ML}) acting on a proximal position can be seen in Figure 5.4. The vertical distance a between the two locations is also marked in the figure. Forces acting on a rigid body can be transformed to another location in the body,

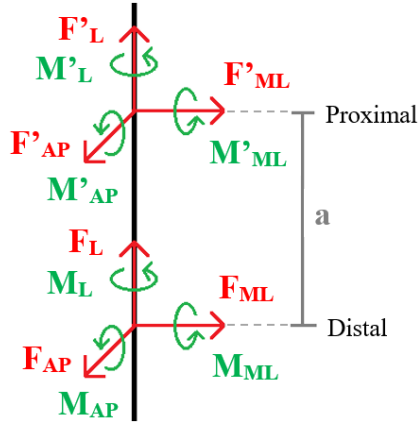


Figure 5.4: An illustration of the coordinate system at a distal (left) and a proximal (right) position in the same rigid body. The six force and moment components are shown for both coordinate systems. The vertical distance between the coordinate systems is a .

and the force will still have the same magnitude. However, if they are moved perpendicularly to their action line, they will also give rise to a moment [27]. This transformation results in the relationships between the force components in the coordinate systems described by Equation (5.1) - (5.3).

$$F'_{AP} = F_{AP} \quad (5.1)$$

$$F'_L = F_L \quad (5.2)$$

$$F'_{ML} = F_{ML} \quad (5.3)$$

Since the force in the long axis direction, F_L , is moved along its action line, it will not cause any additional moment [27]. Therefore, M'_L is described by Equation (5.4).

$$M'_L = M_L \quad (5.4)$$

The other two moments do however change, because of the contribution from the two forces that are moved parallel to their action line: F_{AP} and F_{ML} . M'_{AP}

is a summation of M_{AP} and the moment created by F_{ML} and the distance a , which results in the relationship in Equation (5.5).

$$M'_{AP} = M_{AP} + F_{ML} \cdot a \quad (5.5)$$

M'_{ML} is a summation of M_{ML} and the opposing moment created by F_{AP} and the same distance a , resulting in Equation (5.6).

$$M'_{ML} = M_{ML} - F_{AP} \cdot a \quad (5.6)$$

5.4.2 Transformation of coordinate systems

All loads calculated by OpenSim were originally expressed in the default coordinate frame of the implant body, which is illustrated in Figure 5.5. To enable comparison with the article by Lee et al. [16] and Stenlund's load cell data, the OpenSim data as well as the load cell data were altered to fit the coordinate system used by Lee et al. The positive-negative directions of the medio-lateral axis in the OpenSim system and the antero-posterior axis in the load cell system were changed, and the axes were renamed to resemble the nomenclature used in the article. The aim of this was to transform the data to the coordinate frame presented in Figure 5.6, which has the same axis names and directions as Lee et al. use. The only difference is the placement of origo, which in the article is located in the centre of the load cell, while it in this system is positioned at the point of the abutment for which the OpenSim results are expressed.

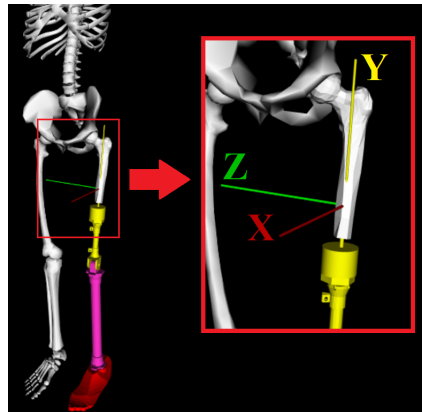


Figure 5.5: Screenshot from OpenSim 3.3 of the coordinate system of the implant body in the OI models. x corresponds to the antero-posterior axis, y to the long-axis and z to the medio-lateral axis.

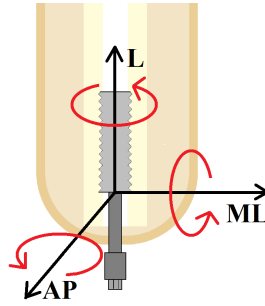


Figure 5.6: Illustration of the coordinate system based on the article by Lee et al. [16], which the results from OpenSim and the load cell are presented in. Positive directions are anterior (AP), proximal (L), and lateral (ML). The red arrows indicate the positive directions of the moments acting about each of the axes.

5.5 Equivalent stress calculations

To analyse the forces and moments that were determined from the JR analyses of the OI models, and study their impact on the implants, the maximum equivalent stresses in the abutment were calculated. The same calculations were also performed on the load cell data received from P. Stenlund. In order to do this, the produced normal and shear stresses had to be evaluated first. For these calculations a solid cylindrical beam was used as a simplified model of the abutment and the abutment screw.

Normal stress

The stress in a cross section of a solid cylindrical beam created by axial forces acting along the axis perpendicular to the surface, and/or bending moments acting around the other two orthogonal axes, is called normal stress, σ [28]. To calculate the normal stress caused by an axial force, σ_n , Equation (5.7) is used:

$$\sigma_n = \frac{F}{A} \quad (5.7)$$

where A is the cross-sectional area on which the axial force F acts [27].

The normal stress created by a bending moment, σ_b , is illustrated in Figure 5.7. To calculate this stress, Equation (5.8) is used.

$$\sigma_b = \frac{M_b}{I_z} \cdot x \quad (5.8)$$

I_z is the area moment of inertia about the same axis as the bending moment M_b acts about, and x is the distance from the neutral axis of the beam, along the axis in which the stress varies. Depending on the coordinate system and

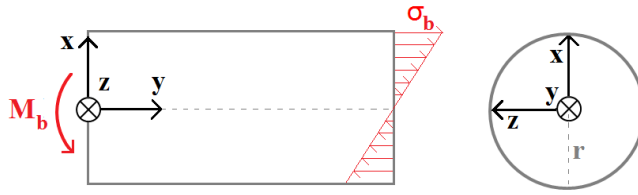


Figure 5.7: The normal stress, σ_b , created by a bending moment, M_b about the z -axis in a solid cylindrical beam, with radius r and length L . The cylinder is illustrated from the side (left) and from the short side (right).

how positive moments are defined, the x coordinate can either be positive or negative. If a positive x generates a positive stress, the sign should be positive. If a positive x generates a negative stress however, the coordinate should be negative. The maximum value of the bending stress occurs at the maximum value of $|x|$, which is at the perimeter of the cross section [27].

For a solid cylindrical beam the area moments of inertia around the two axes in the cross-sectional area, see Figure 5.7, are described by Equation (5.9). In this equation, d is the diameter of the cross section [28].

$$I_x = I_z = \frac{\pi d^4}{64} \quad (5.9)$$

For a beam subjected to both axial forces and bending moments, Equation (5.7) and (5.8) can be combined into Equation (5.10), to calculate the total sum of the normal stresses.

$$\sigma = \frac{F}{A} + \frac{M_b}{I_z} \cdot x \quad (5.10)$$

Shear stress

To calculate shear stress, τ , in a cross section of a solid cylindrical beam, shear forces acting parallel to the surface and torsional moments acting about the long axis of the beam, need to be considered. For shear forces, Equation (5.11) is used for calculating the created maximum shear stress ($\tau_{ij \max}$), which is located in the centre of the cross section.

$$\tau_{ij \max} = \mu \cdot \frac{T}{A} \quad (5.11)$$

i indicates the normal to the surface for which the shear force is calculated, and j indicates the direction of the shear force, T , which creates the shear stress. A is the cross-sectional area of the surface, and μ is a coefficient greater than 1, which depends on the geometry of the cross section [27]. For a circular cross section, μ equals 1.33 [29].

The torsional shear stress, τ_t , created by torsional moments is determined from Equation (5.12). This equation calculates the maximum torsional shear stress, $\tau_{t \max}$, for a solid cylindrical beam, which occurs at the greatest possible distance from the neutral axis, i.e. around the perimeter of the cross section.

$$\tau_{t \max} = \frac{M_t}{W_t} \quad (5.12)$$

$$W_t = \frac{\pi \cdot d^3}{16} \quad (5.13)$$

In Equation (5.12), M_t is the torsional moment about the long axis of the beam, and W_t is the torsional section modulus, which is a property depending on the geometry of the cross section. For a circular cross section, W_t is defined by Equation (5.13), where d is the diameter of the cross section [27].

von Mises stress

Normal and shear stresses acting in the same location of a cross section can be combined into an equivalent tensile stress, σ_e , also known as von Mises stress. This can be used to analyse the effect of multiaxial loading, and it is calculated using Equation (5.14).

$$\sigma_e = \sqrt{\frac{1}{2} ((\sigma_x - \sigma_y)^2 + (\sigma_y - \sigma_z)^2 + (\sigma_z - \sigma_x)^2 + 6(\tau_{xy}^2 + \tau_{yz}^2 + \tau_{zx}^2))} \quad (5.14)$$

In this equation σ_x , σ_y and σ_z represent the normal stresses in the cross section, and τ_{xy} , τ_{yz} and τ_{zx} equal the shear stresses [27].

5.6 Determination of test forces

In order to create a loading situation causing both compression, bending and torsion at the cross section described by Figure 5.3, a set up like the one in Figure 5.8 can be used. When applying a test force (F) at an angle (θ) to the abutment, this will result in normal stress (σ_y) as well as shear stress (τ_t) at the cross-sectional area. The equations for the maximum values of these stresses can be seen on the left hand side of the equivalence arrows in Equation (5.15) and (5.16). The normal stress depends on the components of the applied force (F_x and F_y), the moment arms (a and h), as well as the coordinates of the location for which the normal stress has its maximum (x and z). The shear stress depends on the applied force in the x-direction (F_x), the torsional section modulus (W) and the moment arm (a). In these equations, the force F_x and the moment arm a are unknown, as well as the coordinates, x and z , of the maximum stress. F_y and h are however known, since F_y only depends on

the desired amount of compression, and h is based on the dimension of the abutment. The goal is to determine the unknowns, so that the produced normal and shear stresses are equivalent to the desired values for the test. The desired compressive force F_y is known from the OpenSim simulations and the load cell data, and the stresses are based on the results from the calculations presented in section 5.5.

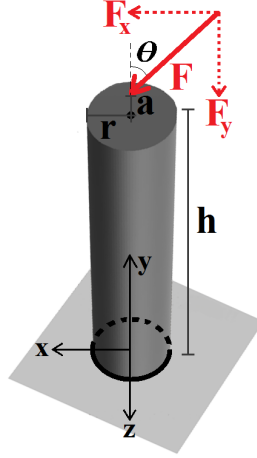


Figure 5.8: Loading situation creating compression, bending and torsion, through application of a single test force (F) at a distance a from the centre of the cross section, and at an angle θ from the normal axis. F can be divided into the two orthogonal components F_x and F_y , r is the radius of the cylinder, and h is its height.

To calculate the magnitude of the applied force and the location for where it should be applied, both Equation (5.15) and (5.16) were solved for F_x , see the right hand side of the equivalent arrows. These expressions for F_x were then set equal to each other and from this a quadratic equation of a was resolved, see Equation (5.17). In Equation (5.18), the resulting expression for a is presented.

$$\sigma_{y \max} = \frac{F_y}{A} + \frac{a \cdot F_y}{I} \cdot z + \frac{h \cdot F_x}{I} \cdot x \iff F_x = \frac{I}{h \cdot x} \left(\sigma_y - \frac{F_y}{A} - \frac{a \cdot F_y \cdot z}{I} \right) \quad (5.15)$$

$$\tau_{t \max} = \frac{F_x \cdot a}{W} \iff F_x = \frac{\tau_{t \max} \cdot W}{a} \quad (5.16)$$

$$a^2 + a \left(\frac{I}{A \cdot z} - \frac{I \cdot \sigma_y}{F_y \cdot z} \right) + \frac{\tau_{t \max} \cdot W \cdot h \cdot x}{F_y \cdot z} = 0 \quad (5.17)$$

$$a = -\frac{1}{2} \left(\frac{I}{A \cdot z} - \frac{I \cdot \sigma_y}{F_y \cdot z} \right) \pm \sqrt{\frac{1}{4} \left(\frac{I}{A \cdot z} - \frac{I \cdot \sigma_y}{F_y \cdot z} \right)^2 - \frac{\tau_{t \max} \cdot W \cdot h \cdot x}{F_y \cdot z}} \quad (5.18)$$

Since Equation (5.18) can be solved for various different combinations of x and z , MATLAB was used to loop through all possible combinations of these. Since it is known that the maximum stress will occur at the perimeter of the cross section, only the combinations of x and z occurring there were included in the calculations. A total of 20 different combinations were tested, which resulted in 40 different possible values of a . These were then inserted back into the right hand side of Equation (5.15), which resulted in 40 corresponding options for F_x . In order to verify the solutions, all combinations were then tested by determining the torsional shear stress using Equation (5.16), to see that it corresponded to the desired value. Finally, one combination of a and F_x were selected based on two criteria: a should be short enough to make the test set up realistic, and F_x should be as low as possible. When both parameters had been selected, F and θ could easily be calculated using the Pythagorean theorem and simple trigonometry.

6. Results

6.1 Literature study

From the literature study, some important matters were brought into the development of the test standard. The first was that the abutment can fail mechanically due to fatigue after extensive use, and that the fatigue life can be determined by applying a cyclic load [16]. According to Lee et al., there is no statistically significant difference in loading of the abutment between the following cyclic activities: straight-line level walking, ascending and descending stairs, ascending and descending a ramp, and walking around a circle [30]. There are however high subject-to-subject variability in the loads applied to the implant, which can be due to different individuals using different walking strategies [16].

In addition to fatigue, mechanical failure of the abutment has also occurred because of the amputee falling [16], and according to Welke et al., falling is rather common. Around 50 % of lower extremity amputees suffer from at least one fall per year, and the highest risk for damaging the implant or implant-bone interface comes from torsional loading, although bending moments might also pose a risk [31].

Another issue to consider when designing the test standard is that an abutment that is too compliant might risk fracturing and transferring the impact onto the fixation, or bending too much which might make attachment and detachment of the prosthesis difficult. A too stiff abutment on the other hand might increase the risk of fracturing the femur or the implant-bone interface, since the load is transferred directly onto the residuum [4].

Prosthetic alignment, i.e. the positioning of the prosthetic foot relative to the residual limb, should also be acknowledged. This will not only affect walking ability, but also change the load transferring from the ground reaction force to the implant [30].

6.2 Review of ISO standards

The standard that has been developed in this Master's project, see chapter 8, is partially based on ISO 7206-4:2010, ISO 7206-6:1992 and ISO 10328:2006. The first two are part of ISO 7206, a group of standards which was chosen due to the similarities in behaviour between implants used at a transfemoral amputation and implants used in total hip replacement [20]. ISO 7206 is divided into different parts and for this project part 4 and part 6 were found relevant, since they discuss endurance testing of the femoral components. The third standard, ISO 10328:2006, was chosen to find out what kind of loads need to be tested to simulate the load bearing in a lower limb during daily activities.

6.2.1 ISO 7206-4:2010

Implants for surgery – Partial and total hip joint prostheses – Part 4: Determination of endurance properties and performance of stemmed femoral components.

ISO 7206-4:2010 describes a test method for determining endurance properties of stemmed femoral components used in total or partial hip joint prostheses, through a cyclic test method. The two parameters endurance limit F_D and endurance cycles N_D are defined, and these need to be specified for cyclic tests. Since the OPRA implant is also subjected to a cyclic load through gait cycles, an endurance test like the one specified in this standard should be considered for the development of the new standard.

Test conditions and how the specimen is set up prior to testing are also defined in ISO 7206-4:2010 [32]. By partially embedding the specimen in a solid material, e.g. acrylic bone cement, it is possible to resemble the loss of bone support while performing the tests [33]. This test condition represents a situation where the prosthesis has become loosened in the femur [34], and this is also considered in the developed standard for the OPRA implant system, since it should mimic a worst case scenario. Another test condition involves a test fluid, 9.0 g/l solution of analytical grade sodium chloride (NaCl) in distilled or deionized water of grade 3, that is used for modular specimens to study wear [33]. The OPRA implant also consists of different components, and therefore this fluid has been included in the developed standard as well. In addition to these specifications, the size of the test batch needed for satisfaction of the standard is also defined. For these tests the batch is set to six specimens [32].

In ISO 7206-4:2010, apparatus used to set up the specimen are also described [32]. These include a gripping device that is used to hold the specimen in position during embedding, and a specimen holder which encloses the embedding

material and the test fluid. These tools were found useful for the developed standard, but had to be modified to fit the shape of the implant and to be able to mount the implant in the desired way. The testing machine and means of loading the specimen are also apparatus specified in ISO 7206-4:2010, and the requirements for these have been used as a base for describing the same properties in the developed standard.

Beyond the findings described above, some of the section titles used in this ISO standards have also been considered for the developed standard. These include: Scope, Terms and definitions, Test principle, Materials, and Apparatus.

6.2.2 ISO 7206-6:1992

Implants for surgery – Partial and total hip joint prostheses – Part 6: Determination of endurance properties of head and neck region of stemmed femoral components.

ISO 7206-6:1992 specifies a test method for establishing the endurance properties of the head and neck region of stemmed femoral components of hip joint prostheses. The methods described here are based on the earlier parts of ISO 7206: part 3 and 4. The main difference from part 4 is that the specified test conditions in ISO 7206-6:1992 are intended to represent a firmly fixed prosthesis, and it might therefore not represent a worst case scenario [34]. After reviewing this standard, the content was therefore not found useful for the development of a standard for the OPRA implant system, since it did not contribute with any additional information compared to part 4 of the same standard.

6.2.3 ISO 10328:2006

Structural testing of lower-limb prostheses – Requirements and test methods.

ISO 10328:2006 describes requirements and test methods for lower limb prostheses. To test the prostheses, both static and cyclic strength tests are performed. The static test simulates the worst loading scenario produced during any activity, meanwhile the cyclic test relates to the loading occurring during normal walking and tests fatigue [35]. Both types of test are suitable for the OPRA implant system, since both scenarios are likely to produce stress in the implant.

In ISO 10328:2006, proof strength and ultimate strength are defined for the static tests, and these have been considered in the developed standard. The need of a separate static torsional test is also expressed in ISO 10328:2006. The user of a prosthesis might apply a twisting load that exceeds the levels of

the twisting moments that are produced in the other structural tests, and this could therefore be tested in a separate test only including a torsional load [35]. This separate torsional test has also been taken into account when developing the standard for the OPRA system.

The cyclic tests described in this ISO standard simulate the maximum loading conditions occurring at different instants during the stance phase of walking. Similarly to what was described in the test procedure in ISO 7206-4:2010, a specific test load is applied to mimic the load conditions, and in ISO 10328:2006 this test load produces axial compression, shear forces, bending moments and/or torque [35]. These loading conditions have also been considered for the cyclic tests of the OPRA implant system.

6.3 Data analyses: OpenSim simulations and load cell data

From the gait simulations that were performed in OpenSim using the OI models, six force and moment plots were generated from the Joint Reactions analysis. These plots are presented in Figure 6.1a) - 6.6a), and show all the forces and moments acting on the implant for all three amputation levels throughout the gait cycle. A vertical dotted black line in each of the plots indicates the border between the stance and swing phases.

As described before, Stenlund's load cell data has been used for comparison with the OpenSim results. In order to enable this, the data was processed according to what is described in section 5.4. This resulted in force and moment plots similar to those created from OpenSim, and they are presented in Figure 6.1b) - 6.6b).

The plots have, as mentioned in 5.4.2, been given the same nomenclature as those in the article by Lee et al. This results in that the motions caused by the bending moments M_{AP} and M_{ML} are referred to as medio-lateral rotation and antero-posterior rotation. M_L , which is a torsional moment, is said to cause internal-external rotation. The directions of these moments correspond to those illustrated in Figure 5.6.

6.3.1 Force components

F_{AP} - in the antero-posterior direction

Figure 6.1a) and b) show the force component acting in the direction of the antero-posterior axis, F_{AP} . Positive forces are directed anteriorly, while negative forces are directed posteriorly. The same curvature can be seen in the plot

from OpenSim and the plot from Stenlund’s load cell data. There are two peaks in both plots, one negative and one positive. The negative posterior peak occurs right after heel strike, during loading response, while the positive anterior peak represents the terminal stance phase occurring just before toe-off. As can be seen in Figure 6.1a) from OpenSim, the implants called mid and low experience approximately the same antero-posterior force throughout the gait cycle, while the high amputation implant deviates from the others. The high amputation has the highest posterior peak, and the lowest anterior peak. Stenlund’s load cell data show some slight deviation between individuals; however, compared to the values in the OpenSim plot, both the anterior and posterior peak are smaller for all load cell subjects.

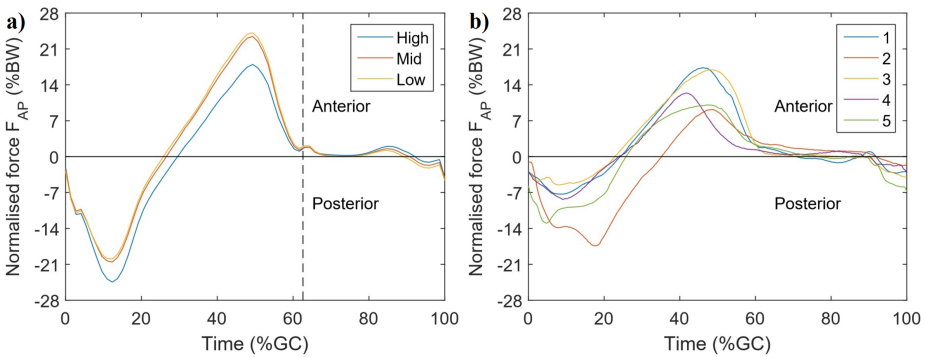


Figure 6.1: Forces acting in the antero-posterior direction on the abutment according to a) the OpenSim simulations and b) the load cell data.

F_L - in the long axis direction

The force acting in the direction of the long axis of the implant, F_L , is plotted in Figure 6.2a) and b). This is the largest of the force components, with peaks up to 100 %BW. In both the OpenSim and the load cell data, the force is consistently positive throughout the stance phase, which means that it is a compressive force. During the swing phase however, there is a small negative force acting on the implants, meaning that they are exposed to a tensile force. In the plot from OpenSim, Figure 6.2a), the highest value of F_L is found in the high amputation, continuously throughout the gait cycle, even though the difference from the other two amputation levels is small. Similarly to what could be seen in the results for F_{AP} , the long-axis force has two peaks: during loading response and terminal stance. This can also be seen in most of the results from the load cell, Figure 6.2b). However, the values of F_L from the load cell are generally lower than the OpenSim values, even though the implant in subject 2 experienced a load of approximately the same magnitude as the OI models.

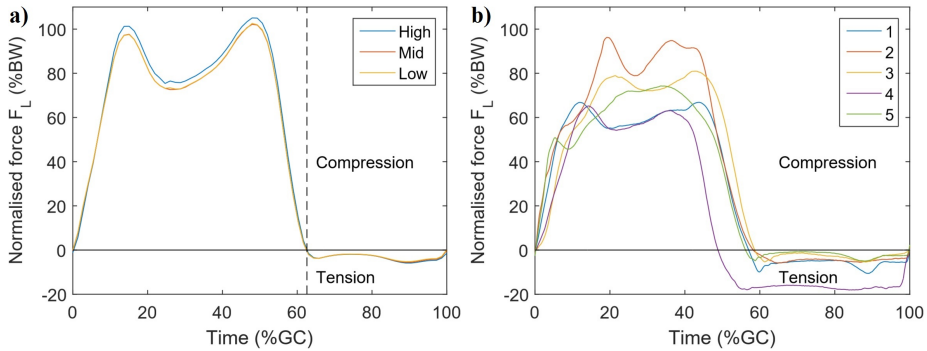


Figure 6.2: Forces acting in the long axis direction on the abutment according to a) the OpenSim simulations and b) the load cell data.

F_{ML} - in the medio-lateral direction

Figure 6.3a) and b) show the force acting in the medio-lateral direction, F_{ML} . For both the OpenSim results and the load cell data, this force is directed laterally throughout the whole stance phase. Similarly to the two other force plots, the OpenSim plot of F_{ML} also shows two peaks during stance phase. Persistently throughout the gait cycle, the mid amputation implant experiences the highest medio-lateral force, while the high amputation implant experiences the lowest load. What is also consistent with the other force plots is that most of the data collected with the load cell show lower values than those from OpenSim. There is however one patient from Stenlund's measurements, subject 3, that experienced the highest load in the medio-lateral direction out of all subjects, in both OpenSim and the load cell study.

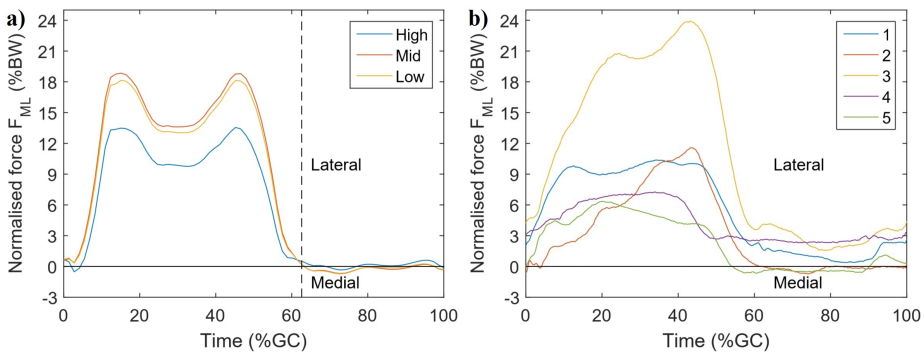


Figure 6.3: Forces acting in the medio-lateral direction on the abutment according to a) the OpenSim simulations and b) the load cell data.

6.3.2 Moment components

M_{AP} - about the antero-posterior axis

The moment acting about the antero-posterior axis of the implant, M_{AP} , is shown in Figure 6.4a) and b). This is the moment causing medio-lateral bending of the implant. In both OpenSim and the load cell data, it is directed laterally throughout the whole gait cycle, except for at the instant of heel strike in the OpenSim plot.

There are two distinct peaks in the OpenSim plot, corresponding to loading response and terminal stance. The terminal stance peak is larger than the loading response peak. The mid and high implant experience approximately the same moment throughout the whole gait cycle, while the low amputation implant is affected by a lower bending moment. Stenlund's load cell data shows some individual variations; some of the subjects only produce one peak, while others show two or three peaks. The OpenSim values are generally higher than the load cell values, as could be seen in the force plots as well. The exception is again subject 3, who experienced approximately the same antero-posterior moment as the low amputation implant in the OpenSim simulations.

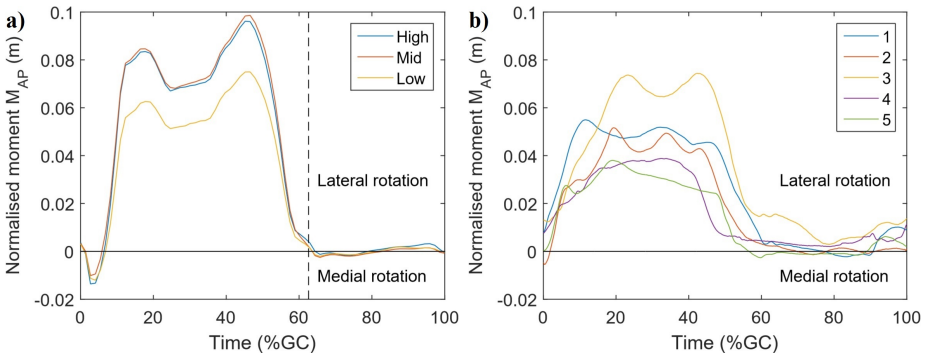


Figure 6.4: Moments applied to the abutment about the antero-posterior axis according to a) the OpenSim simulations and b) the load cell data.

M_L - about the long axis

Figure 6.5a) and b) show the moment acting about the long axis of the implant, M_L . This moment corresponds to torque, and causes internal or external rotation of the implant. There are two peaks in the OpenSim plot: a negative one corresponding to internal rotation during loading response, and a positive one during terminal stance representing external rotation. There are some variations between the implants, but the mid implant shows both the greatest negative and positive peak. The plot from the load cell data shows a wide subject-to-subject

variability. Several peaks can be seen for each subject during the gait cycle and some subjects only experience internal rotation, while others experience both external and internal.

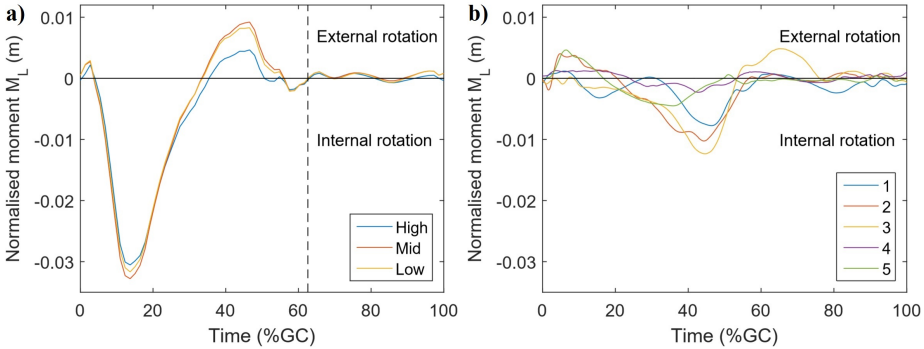


Figure 6.5: Moments applied to the abutment about the long axis according to a) the OpenSim simulations and b) the load cell data.

M_{ML} - about the medio-lateral axis

The moment acting about the medio-lateral axis of the implant, M_{ML} , is plotted in Figure 6.6a) and b). This is the moment causing antero-posterior bending of the implant. All three OpenSim models start the gait cycle with a positive peak, indicating an anterior rotation of the implant. The shapes of the curves then vary between the implants, though they all end the stance phase with a negative local extrema, i.e. a moment causing posterior rotation. The curves from Stenlund's data follow a slightly different pattern compared to the OpenSim results. They start off with a plateau in the anterior direction. At about 40-60 %GC, during the terminal stance phase, all subjects experience a change of direction of M_{ML} , resulting in a posterior rotation.

6.4 Equivalent stress calculations

From the OpenSim results as well as from Stenlund's load cell data, the normalised equivalent maximum stresses created in the abutment during gait were evaluated. This was done for each of the three amputation levels in the OI models, and for each of the five patients included in the load cell study. The calculations were performed using the method described in section 5.5. A simplified model of the abutment and abutment screw was used and this is illustrated in Figure 6.7, where the force and moments that were used for the calculations are also defined. Only the distal parts of the abutment and abutment screw, extending out from the fixture, are included in the model. The abutment and abutment

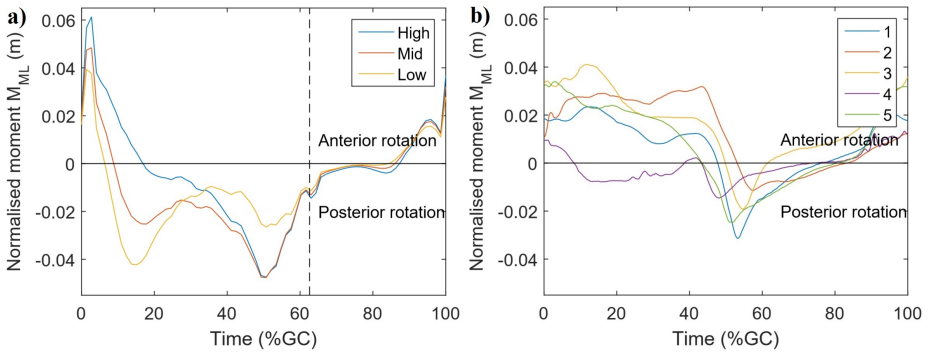


Figure 6.6: Moments applied to the abutment about the medio-lateral axis according to a) the OpenSim simulations and b) the load cell data.

screw are represented as a solid cylinder, neglecting that these are indeed two separate components and that the abutment has an abutment head at the distal end. The cross section where the forces and moments are defined is located in the proximal end of the pictured cylinder, and this is therefore the cross section for which the normal and shear stresses were calculated as well. The diameter of the cylinder used in the model is 11 mm, based on the dimensions of the abutment. In all calculations, the body-weight normalised values of the forces and moments have been used, which results in the stresses having a unit of m^{-2} .

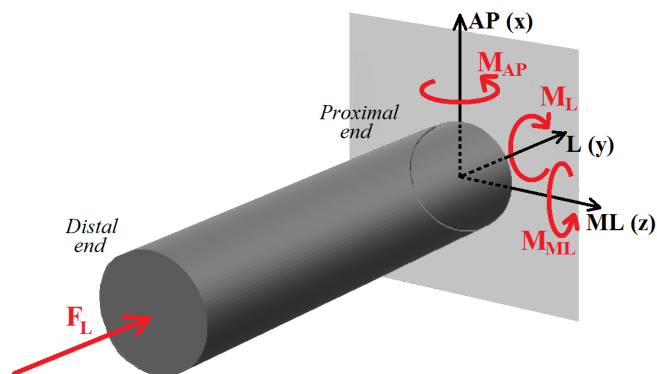


Figure 6.7: The simplified model of the abutment and abutment screw for which the equivalent *Von Mises* stresses have been calculated, based on the illustrated loads. M_{AP} is positive in the lateral rotation direction, M_L external rotation, and M_{ML} in the anterior rotation direction.

As can be seen in Figure 6.7, not all force components have been included in the calculations. Beyond the force and moments defined in the figure there are also shear forces acting in the x- and z-direction: F_{AP} and F_{ML} . Due to their small impact on the equivalent stress compared to the other load components, they have been excluded from this simplified model. This is further explained in section 6.4.2.

6.4.1 Normal stress

In order to evaluate the equivalent stresses in the cross section of each of the abutments and abutment screws, the total normal stresses had to be calculated first. This was done by considering both compression due to the force in the long-axis direction (F_L) and the two bending moments about the medio-lateral (M_{ML}) and antero-posterior (M_{AP}) axes. In the illustrated model in Figure 6.7, the normal stresses acting in the x- and z-direction respectively, are zero. This is due to the fact that none of the bending moments create normal stresses in these directions, and there are no normal forces acting in the x- or z- direction either. There is however a normal stress in the y-direction, σ_y , and this is calculated by using Equation (6.1), which is a combination of Equation (5.7) and (5.8) from section 5.5.

$$\sigma_y = \frac{F_L}{A} + \frac{M_{AP} \cdot z}{I_z} - \frac{M_{ML} \cdot x}{I_x} \quad (6.1)$$

F_L , M_{AP} and M_{ML} are the applied loads causing normal stress in the y-direction, A is the cylinder's cross-sectional area, and I_z and I_x are the area moments of inertia about the z- and x-axis respectively. z and x are the coordinates along the respective axis for the point at which the stress is calculated.

Using MATLAB, Equation (6.1) was implemented for each coordinate of the cross section for each instant throughout the gait cycle. From these calculations Figure 6.8 and Figure 6.9 were created. These figures show the distribution of the normal stresses across the cross-sectional areas, at the time of maximum stress for each of the models and subjects respectively. The location of the maximum values ($\sigma_{y \max}$) in each of the cross sections are indicated with black dots. The magnitudes and times of occurrence are also presented in Table 6.1.

All of the maximum normal stress values, for both OpenSim and the load cell data, are positive, which means that the stress is compressive. The left half of Table 6.1 presents the results from the OpenSim data, and it shows that the mid amputation level generates a higher normal stress in the abutment compared to both the high and low amputation level. For all of the amputation levels, the highest magnitude of normal stress is produced at the same time during the gait

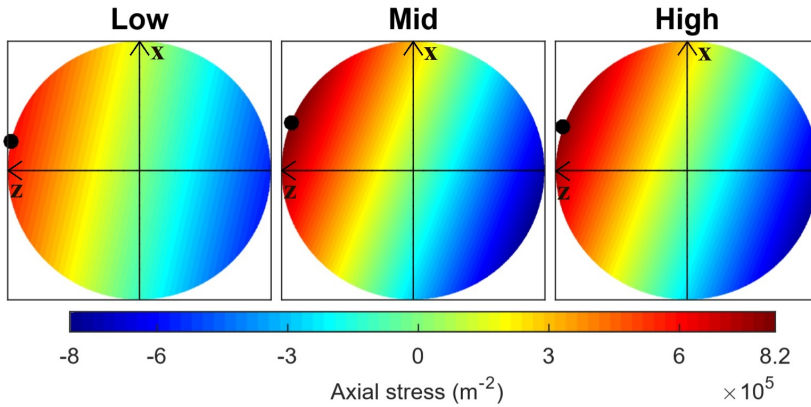


Figure 6.8: The normal stress distribution across the cross-sectional areas of the abutment and abutment screw, at the instant of maximum normal stress, from the OpenSim simulations. Negative values are tensile stresses, and positive values are compressive stresses. The maximum value in each implant is located at the black dot.

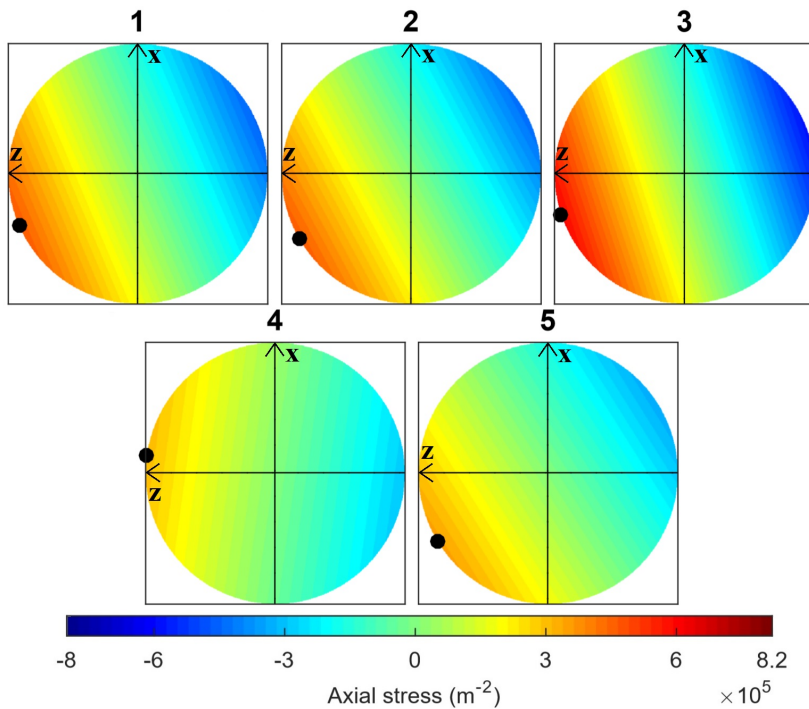


Figure 6.9: The normal stress distribution across the cross-sectional areas of the abutment and abutment screw, at the instant of maximum normal stress, from Stenlund's load cell data. Negative values are tensile stresses, and positive values are compressive stresses. The maximum value in each implant is located at the black dot.

Table 6.1: Normal stress in the abutment and abutment screw at the instant of maximum normal stress, at the coordinates of the cross section subjected to the largest stress.

<i>Model</i>	OpenSim		<i>Subject</i>	Load cell data	
	$\sigma_{y \max} (m^{-2})$	(%GC)		$\sigma_{y \max} (m^{-2})$	(%GC)
Low	$5.99 \cdot 10^5$	46.6	1	$4.65 \cdot 10^5$	11.7
Mid	$8.20 \cdot 10^5$	46.6	2	$4.60 \cdot 10^5$	19.2
High	$7.95 \cdot 10^5$	46.6	3	$6.01 \cdot 10^5$	22.6
			4	$3.07 \cdot 10^5$	32.4
			5	$3.51 \cdot 10^5$	18.9

cycle, at 46.6 %GC. From the plots in Figure 6.1a)-6.3a), this instant appears to be during the terminal stance phase. Another aspect all models have in common, which can be seen in Figure 6.8, is that the maximum normal stress is located on the lateral side of the abutment, anterior to the centre of it.

The right half of Table 6.1 shows the maximum normal stresses based on the load cell data. There are individual differences in the magnitudes of the stresses, but they are all in the same order of magnitude as the values from OpenSim. Subject 3 is however experiencing the highest normal stress out of the load cell subjects. The time of occurrence for these values also varies within the group of subjects, ranging from 11.7 - 32.4 %GC. For all subjects except subject 4, the maximum normal stress is located laterally and posteriorly. The maximum stress in subject 4 is instead located slightly anterior to the centre of the abutment, which can be seen in Figure 6.9.

6.4.2 Shear stress

As with the normal stress calculations, MATLAB was used to implement shear stress calculations for each of the cross sections of the abutment and abutment screw, for each instant of the gait cycle. The maximum values in the cross section of three shear stress components were calculated: $\tau_{yx \max}$, $\tau_{yz \max}$ and $\tau_t \max$. From these calculations, the maximum values in time of each of the components were found. $\tau_{yx \max}$ and $\tau_{yz \max}$ are stresses created by the shear forces in the antero-posterior and medio-lateral directions (F_{AP} and F_{ML}). They were calculated using Equation (5.11), and the results are presented in Table 6.2 and Table 6.3. $\tau_t \max$ is the stress created by the torsional moment M_L , which was calculated using Equation (5.12), and the results are shown in Table 6.4.

Table 6.2: Maximum shear stresses in the abutment and abutment screw due to antero-posterior shear forces ($\tau_{yx \max}$).

OpenSim			Load cell data		
<i>Model</i>	$ \tau_{yx \max} (m^{-2})$	(%GC)	<i>Subject</i>	$ \tau_{yx \max} (m^{-2})$	(%GC)
Low	$3.38 \cdot 10^3$	49.3	1	$2.42 \cdot 10^3$	46.1
Mid	$3.28 \cdot 10^3$	49.3	2	$2.43 \cdot 10^3$	17.5
High	$3.43 \cdot 10^3$	12.3	3	$2.37 \cdot 10^3$	47.9
			4	$1.73 \cdot 10^3$	41.5
			5	$1.82 \cdot 10^3$	4.9

Table 6.3: Maximum shear stresses in the abutment and abutment screw due to medio-lateral shear forces ($\tau_{yz \max}$).

OpenSim			Load cell data		
<i>Model</i>	$ \tau_{yz \max} (m^{-2})$	(%GC)	<i>Subject</i>	$ \tau_{yz \max} (m^{-2})$	(%GC)
Low	$2.54 \cdot 10^3$	15.1	1	$1.45 \cdot 10^3$	34.3
Mid	$2.64 \cdot 10^3$	15.1	2	$1.62 \cdot 10^3$	43.8
High	$1.90 \cdot 10^3$	45.2	3	$3.35 \cdot 10^3$	43.3
			4	$1.02 \cdot 10^3$	33.8
			5	$0.89 \cdot 10^3$	20.1

Table 6.4: Maximum shear stresses in the abutment and abutment screw due to torsion ($\tau_t \max$).

OpenSim			Load cell data		
<i>Model</i>	$ \tau_t \max (m^{-2})$	(%GC)	<i>Subject</i>	$ \tau_t \max (m^{-2})$	(%GC)
Low	$1.21 \cdot 10^5$	13.7	1	$2.96 \cdot 10^4$	46.4
Mid	$1.25 \cdot 10^5$	13.7	2	$3.92 \cdot 10^4$	44.1
High	$1.17 \cdot 10^5$	13.7	3	$4.73 \cdot 10^4$	44.7
			4	$8.72 \cdot 10^3$	42.7
			5	$1.77 \cdot 10^4$	6.7

The coordinates of the three maximum shear stress components were not investigated using MATLAB, as was done for the normal stress, since it is already known that the maximum torsional shear stress will be found around the perimeter of the abutment, and the maximum impact of the shear forces will be found in the centre of the cross section.

The results in Tables 6.2, 6.3 and 6.4 show that for OpenSim, the maximum shear stress created by the torsional moment ($\tau_{t \max}$) is much greater than the stress components produced by the shear forces ($\tau_{yx \max}$ and $\tau_{yz \max}$). Therefore, the two latter can be neglected when calculating the maximum equivalent stress acting on the abutment in the OI-models. For the load cell data, the difference in magnitude between the shear stress components is not as prominent, although the torsional shear stress is still significantly greater than the other two components. In addition, the torsional shear stress is greatest around the perimeter of the cross-sectional area, like the normal stress, while the shear stress components due to shear forces are greatest in the centre. This implies that the maximum equivalent stress is also found around the perimeter of the cross section, and the shear stress components caused by shear forces can therefore be neglected in the calculations for the load cell data as well.

The maximum torsional shear stresses calculated from the OpenSim results are all negative, corresponding to an internal rotation. The mid implant is exposed to the highest stress once again, but it is closely followed by the low and high implant. For all models, this maximum stress occurs at 13.7 %GC. The torsional shear stresses based on the load cell data are not as homogeneous between subjects as those from OpenSim. Subject 1-4 are all exposed to a negative shear stress, while subject 5 is exposed to a positive stress. The time of occurrence also varies; for subject 1-4 this event occurs at about 42-46 %GC, while it is at about 6 %GC for subject 5. Out of the load cell subjects, subject 3 is the one experiencing the highest stress, similarly to what could be seen in the normal stress calculations.

6.4.3 Von Mises stress

As described above, the shear stress caused by torsion is located around the perimeter of the cross section, like the maximum normal stress. It is therefore possible to add these two stress components together to create an equivalent stress, using von Mises equation. This was described in section 5.5 as Equation (5.14). For the loading situation illustrated in Figure 6.7, there is only one normal stress component ($\sigma_{y \max}$) and one shear stress component ($\tau_{t \max}$). Therefore, Equation (5.14) can in this case be rewritten as Equation (6.2) [28].

$$\sigma_e = \sqrt{\sigma_{y \max}^2 + 3\tau_{t \max}^2} \quad (6.2)$$

Since the maximum values of $\sigma_{y \max}$ and $\tau_{t \max}$, which are presented in Table 6.1 and Table 6.4 respectively, appear at different instants during the gait cycle, it would not be relevant to add these values together using Equation (6.2). Instead, MATLAB was used to apply this equation to each instant during the gait cycle. The maximum equivalent stress was calculated for each instant, by finding the maximum normal stress for each time frame, and adding it together with the maximum torsional shear stress for the same instant, using Equation (6.2). From this, the maximum equivalent stress throughout the gait cycle could be found, and the results are plotted in Figure 6.10a) and Figure 6.10b), for OpenSim and the load cell data respectively. In Table 6.5, the maximum values of the equivalent stresses are listed for each of the subjects in the OpenSim models and in the load cell study.

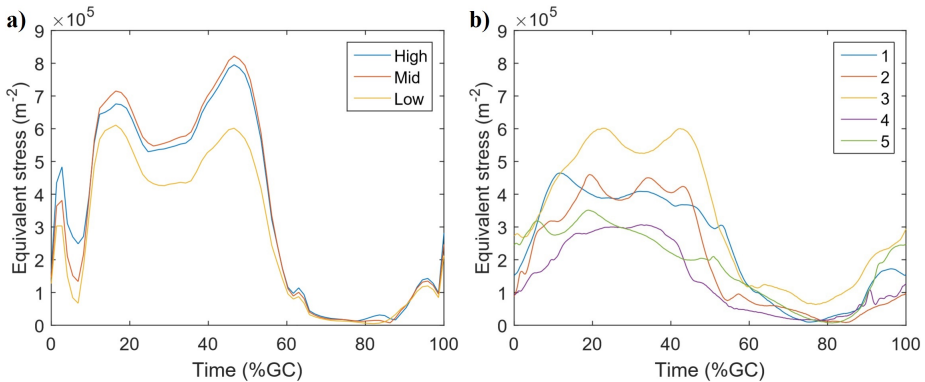


Figure 6.10: Maximum VonMises equivalent stress in the cross section of the abutment and abutment screw, throughout the gait cycle, based on a) the OpenSim simulations and b) the load cell data.

The OpenSim results in Table 6.5 reveal that the mid amputation level is the one experiencing the highest equivalent stress. It is then followed by the high amputation level, and the low is the one experiencing the lowest stress. For the mid and high model, the maximum equivalent stress occurs at 46.6 %GC, while it for the low model occurs at 16.4 %GC. For the load cell data, the values are lower than those from the OpenSim simulations, which can be seen in Table 6.5. The time of occurrence of the event varies between the subjects, from about 11-32 %GC. Subject 3, who also experienced the greatest normal and shear stress, is the one with the highest equivalent stress out of the load cell subjects.

Table 6.5: Maximum equivalent stresses in the abutment and abutment screw.

<i>Model</i>	OpenSim		<i>Subject</i>	Load cell data	
	$\sigma_e (m^{-2})$	(%GC)		$\sigma_e (m^{-2})$	(%GC)
Low	$6.11 \cdot 10^5$	16.4	1	$4.65 \cdot 10^5$	11.7
Mid	$8.22 \cdot 10^5$	46.6	2	$4.60 \cdot 10^5$	19.2
High	$7.95 \cdot 10^5$	46.6	3	$6.01 \cdot 10^5$	22.6
			4	$3.07 \cdot 10^5$	32.4
			5	$3.52 \cdot 10^5$	18.9

6.5 Determination of test forces

From the OpenSim simulations and the load cell data, potential values for the cyclic test force components, and how these should be applied, were determined. This was done by using MATLAB, and the dimensions were based on the dimensions of a real implant. Since the test scenario should test for the worst case scenario, the OI model and load cell subject who experienced the most severe equivalent stress in their respective groups were chosen to base the test values on. The mid amputation level was chosen from the OpenSim simulations and subject 3 was chosen from the load cell data.

As can be seen in Table 6.5, the equivalent stress peaks at 46.6 %GC for the mid model and has a value of $8.22 \cdot 10^5 m^{-2}$. The test values for the mid model were therefore chosen to be based on the stresses that occur at this instant. For subject 3, the equivalent stress has its maximum at 22.6 %GC, during loading response, and peaks at $6.01 \cdot 10^5 m^{-2}$. However, from the equivalent stress plot in Figure 6.10b), it is clear that there is another stress peak of approximately the same magnitude for subject 3. This peak occurs at 42.1 %GC, during stance phase, and has a magnitude of $6.00 \cdot 10^5 m^{-2}$. An important difference between these two peaks is however the contribution from the torsional stress. At the early peak the torsional stress is low, since the torsional moment M_{ML} is only -0.0022 m at this point. At the second peak however, the same moment is instead -0.012 m. Since it has been stated earlier that torsion poses a big risk, it was decided that the stresses that occur at the second peak should be used for determination of test values based on subject 3 instead.

As mentioned before, the aim of the test is to make sure the implants withstand the worst case load. Therefore, a safety margin of 10 % was added to all of the force and moment components included in the equivalent stress calculations, at

the instants described above. The normalised stresses were then recalculated, and these were evaluated for a worst case scenario: a patient weighing 100 kg. This was done using MATLAB. The resulting magnitudes of the desired stresses to be produced in the test are presented below in Table 6.6.

Table 6.6: Desired normal, shear and equivalent stresses in the abutment and abutment screw for the cyclic test, based on OpenSim and load cell data.

Stress type	OpenSim (MPa)	Load cell data (MPa)
σ_y max	885	643
τ_t max	38.0	48.0
σ_e	887	648

Using Equation (5.15) - (5.18) and the method described in section 5.6, the following test parameters were determined for both the mid OI model and subject 3: the endurance limit F_E , consisting of the components F_y and F_x , and a . From the size of the x and y components, the angle θ for application of the test force F_E could also be determined using trigonometry. The values are presented below in Table 6.7. F_y , which is used as an input when solving the other parameters, is equivalent to F_L in the simulations and load cell measurements.

Table 6.7: Values of potential test force parameters for the cyclic test, based on OpenSim and the load cell data.

Parameter	OpenSim	Load cell data
F_y	1086 N	873 N
F_x	-93.9 N	-133 N
a	-10.6 cm	-9.43 cm
F_E	1090 N	883 N
θ	5.0°	8.6°

The value of F_E in Table 6.7 is the force that should be applied to the cross-sectional area of the abutment and abutment screw, at a distance a from the centre, and at an angle θ from the neutral axis, so that the horizontal force component is orthogonal with a . If this is done, the force components F_x and F_y are produced, and the desired levels of normal and torsional stress are obtained.

To simplify the test method, the values from subject 3 have been adjusted to

the ones presented in Table 6.8, since it would be difficult to apply the force at an exact angle of 8.6° . As can be seen in the table, the adjusted parameters produce stresses that are very similar to the original values for the same subject, which can be seen in Table 6.6. The biggest difference is the magnitude of the torsional stress, which is increased by 2.2 MPa. However, since the normal stress is decreased by 1 MPa, the equivalent stress is still the same.

Since the calculated test force and application angle for the OpenSim model can already be considered to be applicable in an actual test, no changes have been made for this model.

Table 6.8: Adjusted test parameters and the stresses they produce, based on the load cell data.

Load cell data			
Stress type	(MPa)	Parameter	
$\sigma_y \text{ max}$	642	F_y	889 N
$\tau_t \text{ max}$	50.2	F_x	-141 N
σ_e	648	a	-9.3 cm
		F_E	900 N
		θ	9.0°

7. Discussion

7.1 Literature study

Apart from contributing to the theoretical background presented in earlier chapters, the literature study has also provided some important and useful insights to acknowledge when developing the test standard, chapter 8. These are discussed below.

As described in section 6.1, abutment failure has been observed as a consequence of extensive use. This suggests that a cyclic fatigue test should be performed. Since there according to Lee et al. is no significant difference in the loading magnitude of the implant between straight-line level walking and other activities that are perceived to be more challenging, such as climbing stairs, it should be sufficient to perform the cyclic test for normal gait. When doing this, it is important to consider the fact that different individuals adopt different walking strategies, and have different prosthetic alignment, which affects the loading on their implant. A cyclic test should represent the worst case of walking, i.e. the subject with the highest loads.

Mechanical failure does not only occur because of fatigue, but also due to falling. This indicates that another test is needed, simulating a scenario worse than walking, which does not occur repetitively. This might be falling, but it could perhaps also be stumbling or jumping, which should also produce worse loads than walking. Since all these scenarios are one time loads, a static test could be used to simulate these.

It was suggested by Welke et al. that both torsion and bending pose potential hazards to the endurance of the implants, and both of these loading modes should therefore be considered when designing a test standard. Another issue to consider when designing the test is the fact that the abutment should have an optimal strength, which was also described in section 6.1. It should not be too stiff, nor too compliant. This suggests that different test conditions might be needed: one with a scenario the abutment should withstand, and one in which it is supposed to break.

7.2 Review of ISO standards

Reviewing ISO standards helped in the development of the standard, by contributing to specifying necessary test parameters, as well as how the specimen is set up. It was also helpful in the specifications of the test conditions and test procedure, as well as with deciding the size of the test batch and what test methods to use: cyclic, static and torsion. Apart from the content, it was also helpful to study the structure of the standards. ISO 7206-4:2010 (*Partial and total hip joint prostheses – Part 4: Determination of endurance properties and performance of stemmed femoral components*) was found most useful out of the three, with short and straightforward descriptions and with a step-by-step explanation of the test procedure.

It was at times hard to understand why certain parts of the tests described in the ISO standards need to be performed, or why a certain material is used. There is for example no explanation to why a fluid is used, or what the partial embedding in ISO 7206-4:2010 simulates. The ISO standards that have been used in this project are based on other ISO standards, and apart from that, no other references are mentioned. In an attempt to clarify things regarding the fluid and the partial embedding, the Technical Committee (TC) responsible for ISO 7206-4:2010 was contacted. A short reply explaining the purpose of them both was received, and this information is included in the results in section 6.2.1.

7.3 OpenSim simulations

7.3.1 Force components

The direction and size of the peaks that can be seen in the OpenSim force plots, Figure 6.1a)-6.3a), are highly dependent on the angle of the implant in comparison to the coordinate system of the ground reaction force (GRF) used in the analyses. There is a slight variation to be observed between the high amputation level and the mid and low amputation levels in all of the force plots, and this difference has to do with tilting of the implants, which has been done in order to align them with the residual femurs. Depending on the amputation level the tilting differs. The high implant has been slightly tilted posteriorly in the sagittal plane, unlike the mid and low implants, and it has also been tilted less in the frontal plane. Since the coordinate system of the implant follows the actual implants, the high implant has a coordinate system with a different angle compared to the GRF system, than the mid and low amputation implants do. The impact of the GRF on the three force components will therefore differ between the amputation levels, and thus the tilting of the implant impacts the

magnitudes of the different components in the force plots.

F_{AP} - in the antero-posterior direction

The antero-posterior GRF component is the force of friction, which means that it is directed in the opposite way of the relative movement between the foot and the ground. This force drives the motion forward and prevents slipping in the antero-posterior direction. During loading response, when the foot is moving in the anterior direction relative to the floor, the force of friction is directed posteriorly. During the terminal stance, the movement and force of friction are directed in the opposite way; the movement goes posteriorly and the force is directed anteriorly. This directional shift is what causes the different directions of the F_{AP} , as can be seen in Figure 6.1a).

During loading response in the OpenSim simulations, the posterior tilting of the high implant results in the implant having a greater angle relative to the y-axis of the GRF, compared to the mid and low implants. This in turn results in a greater posterior component for the high implant. In the terminal stance phase however, the tilting of the implant results in a smaller angle relative to the y-axis of the GRF, compared to the mid and low implant. Consistently with the loading response case, this results in a smaller anterior component for the high implant. The explanation for this is that the tilting of the implant affects the contribution of the large y-axis component of the GRF, to the antero-posterior component of the force acting on the implant. Since neither of the low and mid amputation implants have been tilted in the sagittal plane, they have approximately the same angle compared to the y-axis of the GRF throughout the cycle, and therefore experience the same antero-posterior force on the implant.

F_L - in the long axis direction

F_L is consistently compressive throughout the stance phase of the gait cycle, but during the swing phase it switches to a small tensile force, as can be seen in Figure 6.2a). This tensile force is due to gravitation acting on the prosthesis, and since all prostheses and implants are modelled with the same weights in all three OI models, the tensile force is equivalent for all three amputation heights.

In stance phase, the differences between the high, mid and low amputation level again depend on the slight variation in rotation of the implants compared to the GRF system. This rotation can be both due to the tilting of the implants described above, and slight variations in the walking patterns between the models caused by differences such as the distances between the knees.

F_{ML} - in the medio-lateral direction

F_{ML} is directed laterally throughout the whole gait cycle, see Figure 6.3a). This is due to the fact that the foot is consistently placed medially to the implant, creating a lateral reaction force.

Similarly to what was described for F_{AP} , the F_{ML} component in the coordinate systems of the implants in OpenSim will also have a contribution from the much greater y-axis force in the GRF system, due to alignment of the implants with the residual femur in the frontal plane. In addition to this tilting, the total rotation of the implant during gait is also affected by how the models place their prosthetic foot in comparison with the rest of the body, which depends on how it is aligned in the first place. The larger the rotation between the implant and the GRF is, the greater will the contribution of the GRF y-axis force be to the medio-lateral force on the implant. This rotation can be investigated by looking at the hip adduction angle in OpenSim during the two peaks. This angle reveals that the high amputation implant is the most aligned with the long axis of the GRF, resulting in a smaller medio-lateral force component, while the mid amputation implant has the greatest angle compared to the GRF, causing a larger medio-lateral force. The low amputation implant has an angle in between the high and mid implants, which results in that the medio-lateral force is higher than for the high implant, but lower than the mid. As can be seen in the plot in Figure 6.3a), this is persistent throughout the gait cycle.

7.3.2 Moment components **M_{AP} - about the antero-posterior axis**

In Figure 6.4a), the terminal stance peak is larger than the loading response peak. This is due to the fact that the foot is placed more medially to the implant during terminal stance compared to during loading response, which can be observed by looking at the hip adduction angle in OpenSim. This means that there is a longer moment arm during terminal stance, which explains the greater moment.

The low amputation implant is affected by a lower bending moment than the other two implants, due to a shorter moment arm. The mid and high implant experience approximately the same moment, even though they also have different moment arms. This might be explained by the fact that they can also experience different force magnitudes. If the force creating the moment on the mid implant is higher, and the lever arm is shorter, while the high implant experiences a smaller force with a greater lever arm, this can result in equivalent moments.

M_L - about the long axis

What is most noticeable from Figure 6.5a) is the magnitude of the negative peak. This peak is approximately -0.03 m for all three models, which would correspond to a rotational moment of 29 Nm for a patient weighing 100 kg. This is nearly two times what is allowed by the safety-device *OPRA AxorTM II*, described in section 4.3.3, which releases the prosthesis if the rotational moment exceeds 15 Nm. It is therefore not likely that an implant in reality is ever subjected to a moment this large during normal walking. Possible explanations for why the simulations generate a moment this high may include the fact that the OI-models walk with a gait pattern recorded from a non-amputee, and that the strength of the muscles around the hip on the amputated side has not been adjusted.

 M_{ML} - about the medio-lateral axis

The M_{ML} curves from OpenSim can be compared to the antero-posterior bending moments seen in the hip and knee joint in literature [6]. The variation of the moment acting on the low amputation implant during the gait cycle is similar to the shape of the moment acting on a normal knee joint, while the high amputation implant is more similar to the moment seen at the hip joint. The moment acting on the mid amputation implant is somewhere in between the shape of the hip and knee moments. This seems reasonable considering the different implants' proximity to the two joints.

7.3.3 Equivalent stress**Normal stress**

In the normal stress calculations for the OpenSim results, the mid amputation level experiences the highest stress, followed by the high and low amputation level, see Table 6.1. Considering that the normal stress is based on F_L , M_{AP} and M_{ML} , the size of these will decide the magnitude of the stress. The maximum normal stress occurs at 46.6 %GC, for all three OI-models, and at this instant the moment about the medio-lateral axis is smaller for the low implant compared to the mid and high implant, see Figure 6.6a). The bending moment about the antero-posterior axis is also smaller for the low implant compared to the mid and high, see Figure 6.4a). The magnitudes of these two moments impact the normal stress, resulting in a lower stress for the low implant.

The difference between the mid and high implant is small in all three components: F_L , M_{AP} and M_{ML} . The mid implant does however experience a slightly greater bending moment about the antero-posterior axis, and since the moment components have a greater impact on the normal stress due to their

magnitudes, this results in that the mid amputation level experiences a greater stress. Therefore, a mid amputation level, at the point of terminal stance, seems to be the scenario that produces the highest normal stress in the abutment.

Shear stress

Since it has already been established that the shear stress caused by shear forces, $\tau_{yx \max}$ and $\tau_{yz \max}$, can be neglected when calculating the equivalent stresses, these have been left out from any further discussion.

The torsional stress $\tau_t \max$, see Table 6.4, depends on the torsional moment M_L , which can be seen in Figure 6.5a). Since the mid model is the one experiencing the highest torsional moment it is also the one with the highest torsional shear stress. However, since the torsional moment is considered too high to be realistic for all three models, as discussed in section 7.3.2, the torsional shear stress is also likely to be unrealistically high.

Equivalent stress

The calculated maximum equivalent stresses, see Table 6.5, reveal that the different models experience the worst stress at different instants during the gait cycle. The equivalent stress peaks during terminal stance for the mid and high models, while it peaks during loading response for the low model. For the mid and high models, the peak occurs at the same time as the maximum normal stress, at 46.6 %GC. The normal stress has a greater impact than the torsional stress in the equivalent stress calculations, due to its higher magnitude, and therefore the equivalent stress peaks at the exact same time as the normal stress does for these two models. The low model however, peaks at 16.4 %GC during loading response. The different occurrences in time is due to the impact of two moments: M_L and M_{ML} , see Figure 6.5a) and 6.6a) respectively. For the low model, M_{ML} impacts the normal stress so that it is almost as high during loading response as the maximum value, which occurs during terminal stance. This in combination with a maximum shear stress, caused by M_L , occurring during the same period, results in a maximum equivalent stress occurring during loading response for the low model.

The mid amputation level is the one experiencing the highest equivalent stress, which is not unexpected since it has both the greatest normal and shear stress. This result suggests that the mid amputation would represent a worst case scenario, regarding the stress situations.

7.4 Comparison: OpenSim, load cell, and article data

The results from the OpenSim analyses were compared to the load cell data presented in section 6.3, and to the article by Lee et al. from 2008 [16], as described in section 5.4. The OpenSim force components in Figure 6.1a)-6.3a) were compared to the load cell force components in Figure 6.1b)-6.3b) in this report, and to the graphs in Fig. 3 in the article. The OpenSim moment components in Figure 6.4a)-6.6a) were compared to the load cell data in Figure 6.4b)-6.6b), and Fig. 4 in Lee et al. When comparing the results, it is important to remember that there is some divergence between the subjects in both the load cell data and the article. This depends on the walking pattern of each individual and how they place their foot relative to the knee and hip, as well as how the prosthesis is aligned. These aspects need to be considered when looking at the OpenSim results, which only show one single gait pattern, with one prosthetic alignment. Another important matter to have in mind for the comparison is the fact that the data in Lee et al. is collected in the centre of their load cell, inferior to the actual implant, and it has not been recalculated for the abutment as was done with the load cell data from Stenlund.

7.4.1 Force components

All of the force component plots from the OpenSim analyses have the same shape during the gait cycle as the corresponding load cell components, and the data presented in the article. However, the magnitudes of the different force components varies, as does their consistency between the OpenSim analyses, the load cell data and the article. F_{AP} has peaks at around ± 15 to 25 %BW in the OpenSim simulations, around -18 to -5 and 9 to 17 %BW in the load cell data, and around -15 to -4 and 3 to 21 %BW in the article. The simulated force is in other words slightly greater than both the load cell data and what was measured and presented in the article. A possible explanation for this could be the fact that the OpenSim models are based on normal gait, as is further described in section 7.5. It is likely that amputees take shorter strides than healthy subjects, due to reduced hip mobility and muscle strength, and this will naturally affect the forces and moments acting on the implant. From this perspective, it could be said that the OpenSim models represent a worse case than the measured data.

When it comes to F_L , this component is quite similar in all three data sets, with peaks at around 100 %BW in the simulations, between 60 and 100 %BW in Stenlund's load cell data, and between 72 and 105 %BW in the study by Lee et al. It is worth noting that patient 4 in Stenlund's data set, which is the subject with the lowest peaks at about 60 %BW, experiences a significantly higher

tensile force during stance phase than the other subjects. As mentioned before, this tensile force is due to gravitation acting on the prosthesis. A tensile force of about $-18\%BW$ corresponds to a load of 110 N for subject 4, which means that the prosthesis should weigh about 11 kg. This seems high compared to the data that could be found for the patient's prosthetic knee and foot. It is therefore believed that the load cell might have been set to zero in a different way for this patient, perhaps due to it being an early measurement. If this is the case, this also explains the low magnitude of the positive peaks for this patient.

For F_{ML} , the simulations generated peaks of around 13 to 18 %BW, while the load cell data shows maximum amplitudes between 6 to 24 %BW, and 5 to 23 %BW for the article. As with F_L , the values obtained for F_{ML} from OpenSim thus seem to be reasonable, although the subject-to-subject variability is large in both the article and in the load cell data.

7.4.2 Moment components

The moment plots for the load cell data and from Lee et al. show a greater variability between subjects than the moment plots from the OpenSim simulations do. This is due to the fact that different individuals adopt different walking strategies, and have different muscle strength. For this reason the number of peaks and their positions throughout the gait cycle differ a lot between subjects in measured data. The OpenSim models walk with the same strategy and have identical muscle forces, so there are no differences caused by this in these results.

Another important difference between the OpenSim models and both Stenlund's and Lee et al.'s load cell measurements, which is likely to affect the resulting moments, is the muscle anchoring. In the OpenSim models, all muscles connecting from above the amputated femur and stretching down below the amputation height, have been re-anchored at the distal end of the residual limb. Since the location of the joint where the moments and forces are studied is a few centimetres above this anchoring level, the muscles will have an impact on the calculated moments. This is however not the case for the load cell data, or for Lee et al.'s data, since these measurements are taken approximately 10 cm inferior to the distal end of the abutment. The load cell data is then recalculated to the same level as the OI models, without muscles taken into account, and the article data is unprocessed in this matter.

For all subjects in all data sets, M_{AP} is directed laterally throughout the whole stance phase, except for the OpenSim models who experience a small medial bending during heel strike. This small medial peak might be explained by something occurring in the gait pattern that was used for the OpenSim mod-

els. Apart from this, there are some individual differences that can be noticed in the plots from the load cells. These differences are probably due to the different walking strategies mentioned above and results in some subjects having only one peak, while others have two or even three. Regarding the magnitudes of the moment, the maximum values for M_{AP} in OpenSim were between 0.063 and 0.098 m, while they only reached 0.010 to 0.043 m in the article, and 0.038 to 0.074 m in the load cell data. The explanation for this difference is probably that muscle forces act around the point of measurement in the OpenSim simulations, as well as the fact that the models' walking pattern is based on normal gait.

As described in section 7.3.2, M_L is unrealistically large in the OpenSim simulations, with a normalised peak of approximately -0.030 m. This is a torsional moment, which is caused by rotation of the hip in comparison to the foot, and its magnitude depends greatly on the activation of the muscles around the hip. Therefore, it is likely that this moment varies a lot between amputees and non-amputees, which explains the difference between the results. In both the load cell data and the article, M_L shows large subject-to-subject variability with maximum magnitudes at around ± 0.008 m for the article, and -0.010 m for the load cell data. The measured torque is in other words less than a third of the magnitude of the simulated moment. Again, this might be explained by the fact that the OpenSim models are simulated with normal gait data rather than prosthetic gait, and that the strength of the muscles have not been adopted from the original *Gait 2392* model.

For the final moment, M_{ML} , there are differences between all three data sets. The article shows some subject-to-subject variation in the pattern, although all but three participants generated an anterior rotation peak at about 40 % of the gait cycle, and a posterior rotation peak at about 60 %. The load cell data also show a posterior rotation peak at 50 to 60 %GC, but the anterior rotation peak at 40 %GC are much less prominent. The simulated M_{ML} components are different from both of the measured moments, with different shapes and peaks. The difference in shape might be explained by the location of the point of measurement in relation to muscles, as described before. In OpenSim, the point for which the forces and moments are calculated is surrounded by muscles, while this is not the case for the load cell data, nor for the article data. This could also explain why the magnitude of the simulated M_{ML} is slightly greater than the range of the peaks in both data sets, ranging from -0.05 to $+0.06$ m in the simulations, -0.040 to $+0.038$ m in the article, and around ± 0.03 m in the load cell data.

7.4.3 Equivalent stress

Since the equivalent stresses have only been calculated for the OpenSim results and for the load cell data, the article by Lee et al. is excluded from the following comparison.

Similarly to what could be seen in most of the force and moment plots, the magnitudes of the normal stresses are greater for the OpenSim results than for the load cell data. Subject 3 in the latter data set is the only individual who experienced a normal stress within the same range as the OpenSim models. The explanation for this is that most of the subjects using the load cell were subjected to a smaller F_L and M_{AP} , compared to the OI-models, which in turn resulted in a smaller normal stress. The normal stress calculations also reveal that the maximum values occur at different occasions throughout the gait cycle for different data sets. It takes place during loading response for the load cell data, and during terminal stance phase for the OpenSim simulations. For the load cell data, this is predominantly due to the shape of M_{ML} . Since the peaks in both F_L and M_{AP} are approximately of the same size throughout the gait cycle, the maximum value of M_{ML} decides when the maximum normal stress occurs. For the load cell data, this is during loading response. For the OpenSim models, the occasion for the maximum normal stress depends on the impact of both M_{AP} and M_{ML} . Since both moments peak during terminal stance phase, except for M_{ML} for the low implant, this is also when the normal stress peaks.

The distributions of the normal stresses across the cross-sectional areas in OpenSim are also different, compared to the load cell data. The maximum normal stress is located posteriorly and laterally in the load cell data, except for subject 4, compared to anteriorly and laterally in the OpenSim data. This can be explained by the direction of M_{ML} at the instant of maximum normal stress, which causes anterior rotation in the load cell data, except for subject 4, and posterior rotation in the OpenSim data.

The torsional shear stress results from the load cell also show lower magnitudes than those from OpenSim. This can be explained by the size of the torsional moment about the long axis, M_L , which is much greater in the OpenSim simulations due to the impact of the muscle forces. The shear stress developed in the abutment of subject 3 is the highest among the load cell subjects, which can also be explained by the size of the M_L for this subject. When it comes to time of occurrence of the maximum torsional stress, this varies between the OpenSim models and the load cell subjects. In OpenSim, all maximum values occur during loading response, while most of the load cell subjects experience their maximum during terminal stance phase. These variations are highly dependent on differences in the walking pattern, which was discussed in section 7.4.2.

Since both the normal and shear stresses from the OpenSim simulations are higher than the results from the load cell data, the equivalent stresses are also higher. The maximum equivalent stresses also occur at different locations in time for the OI-models and the load cell subjects. For the load cell subjects the maximum values develop during loading response, compared to the terminal stance phase for the OpenSim simulations. For all subjects in both data sets, but one of the OI-models, this is at the exact same time as the maximum normal stress. Since the normal stress has a greater impact on the equivalent stress than the shear stress, due to the difference in magnitude, it is understandable that the equivalent stresses peak at the exact same time as the normal stresses do. For the low amputation OI-model, which is an exception from this, the explanation was discussed in section 7.3.3.

Subject 3 from the load cell data experienced a greater equivalent stress compared to the rest of the load cell subjects. This individual is also the only one who experienced a stress in about the same range as the OI-models. It is not easy to tell why this subject experienced a greater stress than the rest, but a possible explanation could be different walking strategies and muscle forces. However, this subject can be seen as a worst case scenario within the group of subjects who participated in the load cell study.

7.5 Assumptions and limitations in OpenSim

There are a number of assumptions and limitations to the OpenSim OI models, and the analyses performed on them. These limitations indicate why it might not be appropriate to use the results as exact measurements, but rather use them for analysis of when during the gait cycle the load in different directions is the highest, and compare effects of amputation level. The assumptions and limitations that have been identified for the models created in this project, including the ones associated with the original *Gait 2392* model, are presented below.

Assumptions

- The implant and the connected parts weigh 1 kg in total, independently of the prosthesis length.
- The implant, *OPRA AxorTM II*, and the prosthetic part connecting the device to the prosthetic knee joint, can be modelled as one piece.
- The implant is anchored in alignment with the curvature of the residual femur.
- The implant-femur interface can be modelled as a fixed weld joint with no degrees of freedom.

Limitations

- The marker trajectories that are used for the Inverse Kinematics analysis are based on the *Gait 2392* model, which simulates normal gait rather than prosthetic gait.
- The simulations have been performed using a single gait pattern, while studies have shown large subject-to-subject variability in some of the load components due to different walking strategies.
- The same ground reaction forces have been used for all of the OI models, even though the combined weights of the models' respective bodies are less than that of the *Gait 2392* model, which the GRF is based on.
- The moments of inertia for some of the bodies have either been roughly estimated (implant body, prosthetic tibia and foot) or not changed at all (amputated femur) from the original model.
- The location of the centres of mass for the amputated femur, the implant body, and the prosthetic tibia and foot have been roughly estimated.
- No changes have been made to the strength of the muscles around the amputated femur.
- The remaining muscles in the amputated leg have been anchored arbitrarily to the stump, without detailed knowledge about how this is done in reality.
- The musculotendon actuator model used is a simplification of how muscles work in reality.
- Muscle-tendon parameters are based on experimental data from cadavers [12]. This can vary a lot between individuals.
- The dimensions of the *Gait 2392* model, centres of mass and moments of inertia are based on anthropometric data [12]. Moments and forces will vary not only depending on the mass of the body, which can be normalised, but also depending on for example the lengths of the body parts. Therefore the values received are not necessarily the worst case scenario. A tall person will have longer legs than a short person, creating longer lever arms and therefore greater bending moments.

7.6 Determination of test forces

From the comparison in section 7.4.1 and 7.4.2, it can be concluded that the simulated forces and moments are consistent with the load cell data and the article to some extent, while some of the components differ with a great amount.

The differences are likely to be caused by the assumptions and limitations of the OI models, and the most severe differences are thought to be results of the aforementioned fact that normal gait data has been used for the simulations. Since the OpenSim force and moment components that deviate, as well as the maximum equivalent stresses, are generally higher than the load cell and article data, the simulations seem to represent a worst case scenario. They might however, as has been discussed before, not be realistic, and it would therefore not be relevant to base cyclic test force values on the simulated results. If this would be done, the test force would produce an equivalent stress in the abutment of 887 MPa, which is higher than the fatigue limit specified for the type of titanium used in the implant. As a result of this, if the results from the OpenSim simulations would be realistic, the implants would have to be reconstructed in order to be able to withstand the required test force for 10 million cycles. However, as described before, there are a number of assumptions and limitations indicating that the OpenSim results should not be trusted as numerical values. Therefore, from the two possible test forces presented in section 6.5, the one based on the load cell data has been chosen for the cyclic test in the standard.

The chosen test force produces an equivalent stress of 648 MPa, which is just under the fatigue limit of the implant material. There is therefore no margin for material defects or other weaknesses in the implant, in order for it to satisfy the test standard. The test force is, as was also described in the section 6.5, based on subject 3 in the load cell study, with an addition of a safety margin of 10 % on all force and moment components. This addition is there since there is no way of knowing if the subject is the absolute worst case, or just the worst case out of the five participants. Regarding the number of cycles for application of the cyclic test force, this has been determined to 10 million cycle, based on the current requirement for the implants described in section 4.3.4.

As discussed before, in section 7.1, it would be relevant to perform a static test in addition to the cyclic test simulating gait. The static test should simulate more severe loading events that occur much less frequently than gait, such as falling or stumbling. Depending on the nature of the incident, both high bending loads and torsional loads can occur. The static test should therefore include both of these components. As described in section 6.1 and discussed in 7.1, it would also be beneficial to perform two tests: one with a load the implant should withstand, and one in which the abutment/abutment screw should break, in order to make sure it is not too strong and risks damaging the fixture or residual bone instead. The magnitudes of these test forces will however not be specified in this report, since other simulations and measurements need to be performed in order to determine these loads.

7.7 Ethical reflection

The OPRA implant system can improve the life of an amputee, especially if the individual has experienced problems with the use of a socket prosthesis. The implant is however not suitable for everyone, which can be seen as a loss for the group of patients who can not take part of the technique. The most common cause for lower limb amputation in Scandinavia is peripheral vascular disease, which is often associated with a high mortality and age [17]. This disease is however a contraindication for treatment with osseointegrated prostheses, and therefore this group of patients can not be considered for treatment with the OPRA implant system [15]. Amputations due to non-vascular causes, such as trauma or tumours, are less common. Out of the approximately 2500 major lower limb amputations performed in Sweden annually, only around 70 cases are due to non-vascular causes [17]. Even though it can seem unfair that the technique is only available for such a small part of the patient group, it is the scientific truth, since it is not possible to get osseointegration if the patient is suffering from a peripheral vascular disease.

For the group of patient who can be considered for an OPRA implant, the main target is to help those having problems using conventional socket prostheses, and patients who cannot use them at all. For a patient to be considered a viable candidate, he or she should not weigh more than approximately 100 kg, to ensure that the implant can withstand the load. This criteria, in combination with the objective to foremost help those with socket prosthesis problems, can be considered an ethical dilemma since it therefore is not possible to help all patients.

Another ethical aspect, related to this project, is the static test that should simulate a severe loading situation. As discussed before, the test values for this test have not been specified, due to a limited amount of simulations and test data available on the topic. The reason for that no intentional measurements have been performed on falling subjects using load cells is simple: In order to be allowed to perform a load cell study on amputees, an ethical approval is needed, and it would not be ethical to perform studies of falling since the risk of severe injuries would be too big. Performing simulations is therefore a preferable alternative. The load cell data used in this project however, obtained during normal gait, was originally collected for another study, for which an ethical approval had been received. That approval was granted by the local Swedish Ethical Committee (EPN/Gothenburg Dnr 130-09).

8. The Developed Standard

Based on the results and discussion presented in this report, the following standard for structural testing of implants in transfemoral osseointegrated prostheses has been developed. This is not a complete test standard, but a first attempt to standardise the test procedure of the implants and make it more clinically relevant.

8.1 Scope

This standard establishes a test method for structural testing of osseointegrated implants used for treatment of transfemoral amputees. The test method contains two tests: a cyclic endurance test, and a static test. Relevant terms are defined, the test principle is explained, and necessary materials and apparatus are stated. Finally, the requirements for the test parameters of the endurance test are defined. Methods for examining and reporting the results of the tests are not covered by this standard.

8.2 Terms and definitions

The following terms and definitions apply for this standard:

Endurance limit (F_E)	The magnitude of the cyclic test force, which the implant is required to withstand for the specified number of cycles (N_E) without deforming or breaking.
Endurance cycles (N_E)	The number of cycles during which the cyclic test force (F_E) is applied.
Proof strength (F_P)	A static load that all components of the implant can withstand without deforming or breaking.
Ultimate strength (F_U)	A static load that causes the abutment and/or the abutment screw to deform or break, but leaves the fixture undamaged.

8.3 Test principle

The fixture is partially embedded in a solid medium, so that the embedding material covers the proximal part of it. This is done to simulate bone resorption. It is embedded at an angle from the neutral axis of the implant, to enable production of compression, bending and torque, through application of a single test force. The abutment is inserted and locked in place with the abutment screw, and a fluid medium is then added, covering the exposed distal part of the fixture and the lower part of the abutment. The test procedure then starts with a cyclic test, to determine the endurance properties of the test specimen. A cyclic load that produces axial compression, torsion and bending is applied to the distal end of the abutment. The load is applied until the test specimen fails, or until the specified number of cycles is reached. Without removing the specimen from the embedding medium, it is thereafter examined to see if the loading has caused any defects.

The second part of the test procedure involves a static test, where proof and ultimate strength are investigated. This is done by applying two different static loads, which similarly to the cyclic load causes axial compression, torsion and bending. After the proof load has been applied, the test specimen is examined for defects. If no defects are found, the ultimate strength load is applied, and the specimen is removed from the embedding medium and re-examined. In this case, the aim is to see that the intended damages have occurred, i.e. that the abutment and/or abutment screw have been deformed or broken, while the fixture is undamaged.

A batch of six test specimens is said to satisfy the requirements of this standard if all of the specimens are unbroken after the cyclic test and the static proof strength test, but broken in the described way after the static ultimate strength test.

8.4 Materials

Embedding material

An embedding material is needed for simulating the fixation of the implant in the residual femur. This material must not break due to the load applied in the tests, not display excessive deformation or creep, and have reproducible strength characteristics. An appropriate material is acrylic bone cement.

Fluid test medium

A fluid test medium is needed to cover the top of the fixture and the proximal end of the abutment. This is done to mimic the environment in the human

body, and it enables studies of wear, in addition to the structural tests described in this standard. The fluid could be a 9.0 g/l solution of analytical grade sodium chloride (NaCl) in distilled or deionized water of grade 3, and it should be kept at a temperature of 37 °C throughout the tests.

8.5 Apparatus

Specimen holder

A specimen holder, to be filled with the embedding material and keep the test specimen in the specified direction during testing, is needed. The holder should also be able to contain a layer of the fluid test medium, and its dimensions must suit the test specimens as well as the testing machine. An example of a specimen holder is illustrated in Figure 8.1.

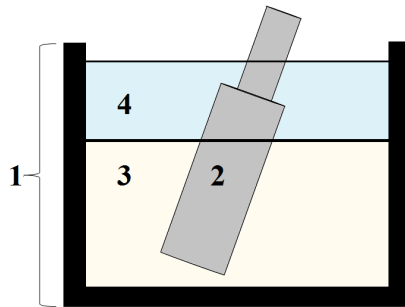


Figure 8.1: Illustration of a specimen holder (1), with a test specimen (2) partially embedded in an embedding material (3), and covered with a fluid test medium (4).

Device to grip the fixture

A device to grip the fixture in its distal end and firmly hold it in place while it is being embedded should be used. Figure 8.2 shows an example of a gripping device. It should be able to grip the device in a predefined angle and it should also be able to adjust the height so that it is possible to lower the fixture into the embedding material.

Means of inserting the abutment

An installation tool is needed to insert the abutment into the fixture.

Torque wrench

A torque wrench is needed to lock the abutment firmly in place using the abutment screw.

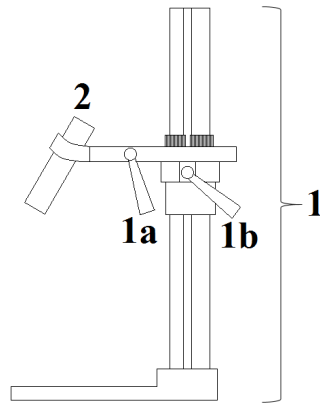


Figure 8.2: Illustration of a gripping device (1) used to hold the fixture (2) in place during embedding. It should be possible to adjust the grip around the fixture (1a) and lower the fixture (1b) into the embedding material.

Testing machine

The testing machine must have the ability to apply both cyclic and static loads, with the magnitudes specified in Table 8.1. There should also be instrumentation available for monitoring and recording the values of the minimum and maximum loads, the corresponding number of load cycles or elapsed time, and the vertical displacement of the test specimen. The machine should also be able to stop automatically if the vertical displacement exceeds a defined value.

Means of loading the test specimen

In order to maintain the loading in the specified direction, means of loading the test specimen are required. The mechanism should allow conversion of the applied test force to production of compression, bending and torque. It should also be of low-friction type, to avoid unintentional forces of friction. Figure 8.3 shows an illustration of a possible loading mechanism, which uses a wedge shaped beam as a lever arm for the applied test load.

8.6 Test parameters

The test parameters concerning the cyclic endurance test are presented in Table 8.1 and illustrated in Figure 8.4. Their specified limits, which are the requirements for satisfying this standard, are also presented in the table. The static proof and ultimate strength parameters are also included in table, even though their values have not been specified, as was explained in section 7.6.

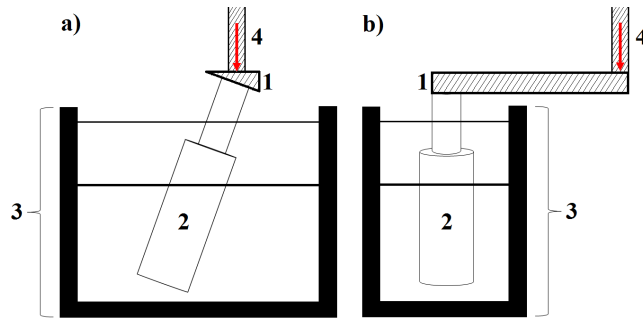


Figure 8.3: Illustration of a loading mechanism, from two perspectives (a and b). The wedge shaped beam (1) creates a lever arm for the loading of the test specimen (2), which is embedded inside the specimen holder (3). The load is applied at the far end of the beam (4).

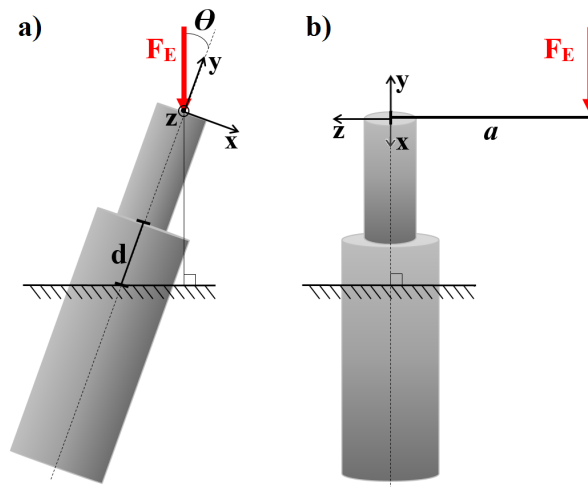


Figure 8.4: A schematic illustration of the orientation of the test specimen (implant) in the cyclic test, and the application of the test force F_E . In a), the specimen is shown from the side where the angle is visible. In b), the specimen is shown from the front where the distance a to the applied force can be seen.

Table 8.1: Test parameters and their specified limits for testing.
N / K stands for not known.

Test parameter		
Designation	Symbol	Limit
Endurance limit	F_E	900 N
Angle for force application	θ	9°
Moment arm from centre	a	9.3 cm
Embedding depth	d	2 - 2.5 cm
Endurance cycles	N_E	10^7
Static proof test force	F_P	N / K
Static ultimate test force	F_U	N / K

9. Conclusions

In this Master's Thesis project, a standard for structural testing of implants in transfemoral osseointegrated prostheses has been developed. This has been done through a literature study, review of ISO standards, gait simulations in OpenSim, and comparison with load cell data. The various parts of the methodology have all contributed to the developed standard, which is not a complete standard for structural testing, but rather a first attempt to standardise the test method. In order to develop a complete standard, and evaluate all parts of it, more time than what was available for this project would have been needed. However, from the results obtained - leading up to the developed standard - it can be concluded that the test requirements posed on the implants today might not reflect the clinical reality. Both the OpenSim simulations and the load cell data used for this standard show higher bending moments for some subjects than what is currently recommended. This suggests that the current test method with its associated requirements, and the method specified in the developed standard, might give different results. It is however difficult to compare the two until the implants have been tested with both set-ups.

Regarding the test set up specified in the developed standard, this has not been tested practically due to lack of time. In order to verify that the test method is feasible, the set up as well as the loading mechanism needs to be verified.

The biggest part of this project has been the development, analysis and validation of the OpenSim osseointegrated models. There is a lot of potential in this type of simulations, and if the models are developed further and the limitations are diminished, they could be used for more detailed studies of the loading on the implant. For example, the aim of determining what amputation level creates the highest stress on the implant was not accomplished in this project, since no general conclusions can be drawn from the performed simulations. This is however something that could be done in case of further development of the OI models.

In the beginning of this project, there were two main goals: to develop a test standard, and to design a functional prototype of a test rig to be used for performing the standardised test. The second goal has however not been fully met, since it has taken more time than what was thought initially to develop the stan-

standard alone. The standard does include illustrations of a concept for how the test rig could be set up, but this has not been specified in detail or tested practically. In order to fulfil the second goal in the future, more work is therefore needed. This is described below, together with further development opportunities based on what has been done in this project.

9.1 Further work

One of the aspects that could be developed further is the use of other ISO standards, as a starting point for the developed standard. As mentioned before, it was at times difficult to understand why certain test conditions, methods, materials, etc. are used in the reviewed standards, since a very limited amount of references are included. Therefore, if more time was available it would have been interesting to establish a better contact with the Technical Committee responsible for the standards, to get to know more about the underlying reasons for each step in them.

To further develop the OpenSim OI models, the first alternative would be to include prosthetic gait data instead of using normal gait data from the *Gait 2392* model. It is likely that the marker trajectories would be different for prosthetic gait, and it would therefore be useful to have gait analysis data from an amputee fitted with an osseointegrated transfemoral prosthesis to use as input instead. Attempts to get hold of this type of data were made in this project, but without success.

An alternative to using prosthetic gait data could be to set restrictions to the joints of the model, based on articles on the topic. There is for example an article by Tranberg et al. [36] which presents a study about differences in hip and pelvic motion between patients with osseointegrated transfemoral prostheses and a control group. Less hip extension ability and lower maximum anterior pelvic tilt was found in the patient group, even though the values changed towards those of the controls from the pre-operative measurements to the two-year follow up. By using the values presented in the article as constraints for the OI models, e.g. restricting the range of the hip extension movement, the gait of the models could be made more similar to that of prosthetic gait. It would however be a more preferable alternative to use real prosthetic gait data instead, if this would be available.

Due to the many limitations to the developed OpenSim models, the test forces in the developed standard were ultimately based on the load cell data received from Stenlund. This data set included five subjects, which is a fairly small group to draw conclusions from, especially regarding worst case scenarios. In

the future, it could therefore be beneficial to perform more studies using load cells, and include more subjects, in order to get a better understanding of what is actually the worst possible loading case during gait. When it comes to other loading scenarios such as falling or stumbling, described before as static, these need to be considered more as well in order to specify appropriate static test forces in the standard. This could potentially be done through simulations, similarly to what has been done in an article by Welke et al. [31].

There are several further developments opportunities regarding the developed test standard. It is not a complete standard compared to the ISO standards, since it for example lacks a detailed description of the test procedure. In order to write such a description, it is however necessary to test the described method practically first, to see if it is feasible. It is also necessary to further specify and test the described apparatus, and if such tests are successful, a more detailed prototype of the conceptual test rig described in the standard can be designed. Ultimately, this rig needs to be tested as well.

Bibliography

- [1] Integrum AB (2016-03-07).
Retrieved from <http://integrum.se>
- [2] Frossard, L., Stevenson, N., Smeathers, J., Häggström, E., Hagberg, K., Sullivan, J., Ewins, D., Gow, D.L., Gray, S. & Brånemark, R. (2008). *Monitoring of the load regime applied on the osseointegrated fixation of a trans-femoral amputee: a tool for evidence-based practice*. *Prosthetics and Orthotics International*, 32(1), pp. 68-78.
- [3] Björnsdóttir, M. (2016-05-11). *Integrum AB*, personal communication.
- [4] Frossard, L. A., Tranberg, R., Haggstrom, E., Percy, M., & Brånemark, R. (2010). *Load on osseointegrated fixation of a transfemoral amputee during a fall: loading, descent, impact and recovery analysis*. *Prosthetics and Orthotics International*, 34(1), pp. 85-97.
- [5] Martini, F.H. & Bartholomew, E.F. (2013). *Essentials of Anatomy & Physiology*, 6th edition. Pearson, USA.
- [6] Backus, S. I., Brown, A. M. & Barr, A. E. (2012). *Biomechanics of Gait*. In: Nordin, M., & Frankel, V. H. (Eds.) *Basic Biomechanics of the Musculoskeletal System*, 4th edition. Lippincott Williams & Wilkins, USA.
- [7] An, Y. H. & Draughn, R. A. (Eds.) (2000). *Mechanical testing of bone and the bone-implant interface*, CRC Press, USA.
- [8] Froes, F. H. (Ed.) (2015). *Titanium: Physical Metallurgy, Processing, and Applications*, ASM International, USA.
- [9] Delp, S. L., Anderson, F. C., Arnold, A. S., Loan, P., Habib, A., John, C. T., Guendelman, E., & Thelen, D. G. (2007). *OpenSim: Open-source Software to Create and Analyze Dynamic Simulations of Movement*. *IEEE Transactions on Biomedical Engineering*.

- [10] SimTK (2016-02-25). *OpenSim*. Retrieved from <https://simtk.org/home/opensim>
- [11] National Center for Simulation in Rehabilitation Research (2016-02-25). Retrieved from <http://opensim.stanford.edu/work/index.html>
- [12] SimTK (2016-02-29). *OpenSim Support*. Retrieved from <http://simtk-confluence.stanford.edu:8080/display/OpenSim/>
- [13] Nebergall, A., Bragdon, C., Antonellis, A., Kärrholm, J., Brånemark, R., & Malchau, H. (2012). *Stable fixation of an osseointegrated implant system for above-the-knee amputees: titel RSA and radiographic evaluation of migration and bone remodeling in 55 cases*. *Acta Orthopaedica*, 83(2), pp. 121-128.
- [14] Gholizadeh, H., Osman, N. A. A., Eshraghi, A., Ali, S., & Yahyavi, E. S. (2013). *Satisfaction and problems experienced with transfemoral suspension systems: a comparison between common suction socket and Seal-In liner*. *Archives of Physical Medicine and Rehabilitation*, 94(8), pp. 1584-1589.
- [15] Hagberg, K., & Brånemark, R. (2009). *One hundred patients treated with osseointegrated transfemoral amputation prostheses—rehabilitation perspective*. *Journal of Rehabilitation Research & Development*, 46(3), pp. 331-344.
- [16] Lee, W. C., Frossard, L. A., Hagberg, K., Haggstrom, E., Gow, D. L., Gray, S., & Brånemark, R. (2008). *Magnitude and variability of loading on the osseointegrated implant of transfemoral amputees during walking*. *Medical Engineering & Physics*, 30(7), pp. 825-833.
- [17] Hagberg, K., & Brånemark, R. (2001). *Consequences of non-vascular trans-femoral amputation: a survey of quality of life, prosthetic use and problems*. *Prosthetics and Orthotics International*, 25(3), pp. 186-194.
- [18] Brånemark, P. I., Hansson, B. O., Adell, R., Breine, U., Lindstrom, J., Hallen, O., & Ohman, A. (1977). *Osseointegrated implants in the treatment of the edentulous jaw. Experience from a 10-year period*. *Scandinavian Journal of Plastic and Reconstructive Surgery*, 16, pp. 1-132.
- [19] Brånemark, R., Brånemark, P. I., Rydevik, B., & Myers, R. R. (2001). *Osseointegration in skeletal reconstruction and rehabilitation: a review*. *Journal of Rehabilitation Research & Development*, 38(2), pp. 175-181.

- [20] Brånemark, R., Berlin, Ö., Hagberg, K., Bergh, P., Gunterberg, B., & Rydevik, B. (2014). *A novel osseointegrated percutaneous prosthetic system for the treatment of patients with transfemoral amputation*. *The Bone & Joint Journal*, 96(1), pp. 106-113.
- [21] Frossard, L., Hagberg, K., Häggström, E., Gow, D. L., Brånemark, R., & Pearcy, M. (2010). *Functional outcome of transfemoral amputees fitted with an osseointegrated fixation: Temporal gait characteristics*. *Journal of Prosthetics and Orthotics*, 22(1), pp. 11-20.
- [22] Integrum AB (2016). *OPRA Implant System for Direct Skeletal Anchoring of Amputation Prostheses - Instructions for Use*.
- [23] Integrum AB (2016). *OPRA AxorTM II - Instructions for Use*.
- [24] International Organisation for Standardization (2016-02-05). Retrieved from <http://www.iso.org/>
- [25] SimTK Public Forums (2016-02-29). *Prosthesis model, posted on 2014-06-03*. Retrieved from <https://simtk.org/forums/viewtopic.php?f=91&t=4926&p=12102&hilit=prosthesis%C2%A8#p12102>
- [26] Stenlund, P. (2015). *On the role of surface properties for implant fixation: From finite element modeling to in vivo studies*. Department of Biomaterials, Institute of Clinical Sciences, Sahlgrenska Academy at University of Gothenburg, Sweden.
- [27] Svensson, I. & Wihlborg, G. (2007). *Mekanik i verkligheten*. KFS i Lund, Sweden.
- [28] Bodelind, B. & Persson, A. (2011). *Hållfasthets- och materialtabeller*. Holmbergs i Malmö AB, Sweden.
- [29] Dahlberg, T. (2003). *Formulas in Solid Mechanics*. Solid Mechanics/IKP, Linköping University, Sweden. Retrieved from http://www.solid.iei.liu.se/Education/formula_table.pdf
- [30] Lee, W. C., Frossard, L. A., Hagberg, K., Haggstrom, E., Brånemark, R., Evans, J. H., & Pearcy, M. J. (2007). *Kinetics of transfemoral amputees with osseointegrated fixation performing common activities of daily living*. *Clinical Biomechanics*, 22(6), pp. 665-673.
- [31] Welke, B., Schwarze, M., Hurschler, C., Calliess, T., & Seehaus, F. (2013). *Multi-body simulation of various falling scenarios for determining resulting loads at the prosthesis interface of transfemoral amputees*

- with osseointegrated fixation*. Journal of Orthopaedic Research, 31(7), pp. 1123-1129.
- [32] International Organization for Standardization (2010). *ISO 7206-4:2010(E) Implants for surgery – Partial and total hip joint prostheses – Determination of endurance properties and performance of stemmed femoral components*. Geneva, Switzerland.
- [33] Zeier, K. (2016-03-21). *DIN Standards Committee Optics and Precision Mechanics*, personal communication.
- [34] International Organization for Standardization (1992). *ISO 7206-6:1992(E) Implants for surgery – Partial and total hip joint prostheses – Determination of endurance properties of head and neck region of stemmed femoral components*. Geneva, Switzerland.
- [35] International Organization for Standardization (2006). *ISO 10328:2006(E) Structural testing of lower-limb prostheses – Requirements and test methods*. Geneva, Switzerland.
- [36] Tranberg, R., Zügner, R., & Kärrholm, J. (2011). *Improvements in hip-and pelvic motion for patients with osseointegrated trans-femoral prostheses*. Gait & posture, 33(2), pp. 165-168.

List of Figures

Figure 1.1	2
"Bone with screw", Copyright by Integrum AB, used with permission (2016-04-22). Retrieved from http://integrum.se/our-solutions/opra-implant-systems/	
Figure 2.1	6
After: "Anatomical Planes", Wikipedia (2016-02-12). Retrieved from https://upload.wikimedia.org/wikipedia/commons/thumb/3/31/Anatomical_Planes.svg/2000px-Anatomical_Planes.svg.png	
Figure 2.2	6
After: "Bones of the leg", Wikipedia (2016-02-05). Retrieved from https://en.wikipedia.org/wiki/Human_leg#/media/File:Human_leg_bones_labeled.svg	
Figure 2.3	7
After: "Fig. 17-2" in: Nordin, M., & Frankel, V. H. (Eds.) <i>Basic Biomechanics of the Musculoskeletal System</i> , 4th edition, p. 429. Lippincott Williams & Wilkins, USA.	
Figure 5.7	28
After: "Fig. 13:9" in Svensson, I. & Wihlborg, G. (2007). <i>Mekanik i verkligheten</i> , p. 185. KFS i Lund, Sweden.	
Figure 8.2	68
After: "Figure A.2" in: International Organization for Standardization (2010). <i>ISO 7206-4:2010(E) Implants for surgery – Partial and total hip joint prostheses – Determination of endurance properties and performance of stemmed femoral components</i> . Geneva, Switzerland.	

All figures not included in the list above have been produced by the authors of this Master's Thesis.